CHAPTER EIGHT

The Role of Body Size Variation in Community Assembly

Samraat Pawar[1]
Grand Challenges in Ecosystems and the Environment, Silwood Park, Department of Life Sciences, Imperial College London, Ascot, Berkshire, United Kingdom
[1]Corresponding author: e-mail address: s.pawar@imperial.ac.uk

Contents

Abstract

Body size determines key behavioral and life history traits across species, as well as interactions between individuals within and between species. Therefore, variation in sizes of immigrants, by exerting variation in trophic interaction strengths, may drive the trajectory and outcomes of community assembly. Here, I study the effects of size variation in the immigration pool on assembly dynamics and equilibrium distributions of sizes and consumer–resource size-ratios using a general mathematical model. I find that because small sizes both, improve the ability to invade and destabilize the community, invasibility and stability pull body size distributions in opposite directions, favoring an increase in both size and size-ratios during assembly, and ultimately yielding a right-skewed size and a symmetric size-ratio distribution. In many scenarios, the result at equilibrium is a systematic increase in body sizes and size-ratios with trophic level. Thus these patterns in size structure are 'signatures' of dynamically constrained, non-neutral

Advances in Ecological Research, Volume 52
ISSN 0065-2504
http://dx.doi.org/10.1016/bs.aecr.2015.02.003

community assembly. I also show that for empirically feasible distributions of body sizes in the immigration pool, immigration bias in body sizes cannot counteract dynamical constraints during assembly and thus signatures emerge consistently. I test the theoretical predictions using data from nine terrestrial and aquatic communities and find strong evidence that natural communities do indeed exhibit such signatures of dynamically constrained assembly. Overall, the results provide new measures to detect general, non-neutral patterns in community assembly dynamics, and show that in general, body size is dominant trait that strongly influences assembly and recovery of natural communities and ecosystems.

1. INTRODUCTION

Understanding general patterns or 'rules' in the dynamics of community assembly is of great theoretical and practical importance and remains one of the foremost challenges in ecology (Bascompte and Stouffer, 2009; May, 2009). In nature, local communities assemble through the dynamics of immigration and species interaction-driven extinction, which exert a 'filter' on all possible interactions given the available species pool for immigration (Bastolla et al., 2005; Pawar, 2009; Post and Pimm, 1983). While this general idea seems intuitive enough, we largely lack empirically testable theoretical predictions for general patterns of community assembly rates and trajectories, or for the types of species traits that are likely to facilitate rapid assembly or reassembly following disturbances (an issue of great practical importance). This is coupled with the problem that empirical data on the temporal sequences of community food web assembly remain scarce (May, 2009, but see Fahimipour and Hein, 2014).

In the context of community assembly, body size is a key trait because it strongly determines colonization rates though it effects on locomotion and dispersal (Hein et al., 2012; Schmidt-Nielsen, 1984), the strength of interspecific trophic interactions following colonization (Pawar et al., 2012; Vucic-Pestic et al., 2010), and life history rates that determine population energetics such as of basal metabolism, intrinsic growth and mortality (Brown et al., 2004; Economo et al., 2005; Kleiber, 1961; Peters, 1986; Savage et al., 2004). These wide-ranging effects of body size raise a suite of interesting and potentially important questions about what role body size variation in the global or regional species pool plays in the rate and trajectory of local community assembly. For example, it would be desirable to know if certain properties of the distribution of body sizes in the

immigration pool can improve or accelerate the rate of community assembly. Yet, only a handful of previous studies have considered the role of size in community assembly dynamics (Etienne and Olff, 2004; Fukami, 2004; O'Dwyer et al., 2009; Virgo et al., 2006). And of these, the subset that have explicitly considered the filtering effects of interaction-driven extinction in food web dynamics (Fukami, 2004; Virgo et al., 2006) have not studied the effects of size variation in the immigration pool on local community assembly dynamics or the resulting local size or size-ratio distributions.

In this paper, I focus on the fact that body sizes in natural communities can span many orders in magnitude (Brose et al., 2006a; Cohen et al., 2003; Jonsson et al., 2005) and study what role the distribution of body sizes in the immigration pool play in dynamics of interaction-mediated local community food web assembly. In particular, by using a general size-constrained mathematical model of food web assembly, I ask whether assembled food webs at quasi-equilibrium (where species numbers remain relatively constant; Bastolla et al., 2005; Pawar, 2009) are expected to show 'signatures' of non-neutral, size-mediated assembly in (i) distribution of body sizes, (ii) distribution of size-ratios between consumers and resources, and (iii) distributions of sizes and size-ratios across trophic levels, and what role the distribution of sizes in the immigration pool plays in all this. I study not just size but size-ratios as well, because, along with consumer size, size difference between consumer and resource strongly determines tropic interaction strength (Pawar et al., 2012; Vucic-Pestic et al., 2010), a key factor driving individual invasion fitness as well as community stability during and after assembly (Brose et al., 2006b; Emmerson and Raffaelli, 2004; Otto et al., 2007; Pawar, 2009; Tang et al., 2014). I then evaluate the theoretical predictions using food web data from nine terrestrial and aquatic communities.

2. THEORY

I use a Lotka–Volterra (LV) type model of biomass dynamics of an n species community (May, 1974; Pawar, 2009; Tang et al., 2014; Virgo et al., 2006) to model food web assembly dynamics (Fig. 1):

$$\frac{dx_i}{dt} = x_i\left(b_i - d_i + \sum_{j=1}^{n} a_{ij}x_j\right), i = 1, 2, \ldots, n \quad (1)$$

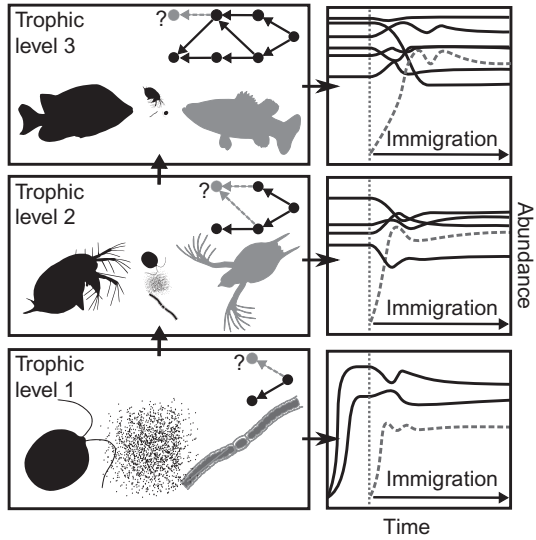

Figure 1 An illustration of the size-constrained community assembly process. At each step of sequential assembly (going bottom to top panel), consumer size and consumer–resource size-ratio determine whether a new immigrant can invade when rare (each dashed line, satisfying the condition in Eq. 20), and then whether the augmented community is stable (the solid lines do not decline to zero, determined by Eq. 24).

Here, x_i is the total biomass of the ith species' population, b_i its intrinsic biomass production rate (0 for consumers) and d_i its intrinsic density-independent biomass loss rate. For the jth consumer and ith resource, coefficient a_{ij} is mass-specific search rate which governs the rate of per-unit biomass loss of the ith species to consumption by the jth species (Pawar et al., 2012). Thus, biomass gain rate of the former (a_{ji}) and loss of the latter (a_{ij}) are related such that,

$$a_{ji} = -ea_{ij}, \text{ (when } j \text{ consumes } i) \tag{2}$$

where e is the consumer's biomass conversion efficiency of the consumer, which does not scale with body mass within major organismal groups or trophic levels (DeLong et al., 2010; Hechinger et al., 2011). Therefore, henceforth I will assume $e = 0.5$, close to the value observed for carnivores. As long as $e > 0$, this paper's results do not qualitatively depend upon it. Finally, the coefficient a_{ii} (when $i = j$ in the sum in Eq. 1) is a mass-specific intraspecific 'search' rate that governs intraspecific interference between individuals of the ith species (DeLong, 2014; Pawar et al., 2012).

As such, Eq. (1) assumes a Type I (linear) functional response of the consumer. As long as most of the a_{ii}'s are non-zero with magnitudes in the order of the a_{ij}'s (i.e. have some level of intraspecific density dependence), using a Type II functional response instead, where consumer handling times for their resource are taken into account, do not change the results of this paper (Pawar, 2009; Tang et al., 2014).

2.1 Size-Scaling Parameterizations

I use the following body size-based parameterizations of the LV model (Eq. 1). In the following scaling relationships, the normalization constants also include the effects of metabolic temperature (Dell et al., 2011; Gillooly et al., 2001; Savage et al., 2004). For biomass production and loss rates, I use

$$b_i = b_0 m_i^{\beta-1} \tag{3}$$

and

$$d_i = d_0 m_i^{\beta-1} \tag{4}$$

where b_0 and d_0 are normalization constants, m is the species' average adult body mass, and $\beta = ¾$. These relationships are empirically well supported (Brown et al., 2004; McCoy and Gillooly, 2008; Peters, 1986; Savage et al., 2004), and have been used previously in similar contexts (Brose et al., 2006b; Pawar et al., 2012; Virgo et al., 2006; Weitz and Levin, 2006; Yodzis and Innes, 1992). For the search rate coefficient between the ith resource and jth consumer species, I use

$$a_{ij} = -a_0 m_j^{-0.25} \varphi_{ij} \tag{5}$$

where, a_0 is a normalization constant, and $\varphi_{ij} \in [0, 1]$ is a dimensionless function that embodies attack success probability. Thus, from Eq. (2):

$$a_{ji} = e a_0 m_j^{-0.25} \varphi_{ij} \tag{6}$$

Note that the quarter-power exponent in Eqs. (5) and (6) has been used for the scaling of search rate in numerous previous studies (Brose et al., 2006b; Otto et al., 2007; Virgo et al., 2006; Yodzis and Innes, 1992). However, according to the results of Pawar et al. (2012; also see Giacomini et al., 2013; Pawar et al., 2013), this is approximately the scaling exponent for 2*D* (two spatial dimensions; e.g. benthic) interactions only. For simplicity, I am thus assuming here that all food webs have

2*D* interactions only (Tang et al., 2014). I will consider the effect of 3*D* or a mixture of 2*D*–3*D* interactions in a subsequent paper.

Next, I assume that attack success probability is unimodal (Gaussian; Fig. 2) with respect to average resource mass (consumer–resource body mass ratio, or size-ratio):

$$\varphi_{ij} = \exp\left(-\left(s\log\left(m_j m_i^{-1}/k\right)\right)^2\right) \tag{7}$$

Here, s determines how rapidly the function reaches its peak k, the size-ratio of maximum consumption rate. This is a simplification of the potentially complex dynamics of consumer–resource encounter and consumption rates in nature, but captures an important feature of empirically observed attack and capture rates—these are unimodal because attack success decreases and handling time increases at extreme size-ratios (Aljetlawi et al., 2004; Brose et al., 2008; Persson et al., 1998). The actual values of k and s are expected to vary with type of consumption (foraging) strategy as well as habitat type. For example, in the case of predator–prey interactions, because smaller consumers have greater mass-specific power relative to larger ones, and can hence handle a larger range of prey sizes, k may be closer 1 (or even <1) for small consumers, and s smaller (a more gradual decline of consumption rate at extreme ratios). Brose et al. (2006a) have shown that invertebrate consumers do indeed have a k closer to 1 than vertebrates across disparate habitat types, suggesting their superior ability to attack and capture prey closer to their own size. In host-parasite and parasitoid interactions on the other hand, k should be <1 because parasites and parasitoids are selected to adopt strategies that increase effective encounter rate as well as exploitation success of resource species much larger than themselves (Cohen et al., 2005; Lafferty et al., 2008; Raffel et al., 2008). Below, I show that my results are largely insensitive over a wide range of choice of the parameters k and s.

Finally, I specify the intraspecific search rate a_{ii}. Because a_{ii} represents biomass loss (including individual mortality) resulting from metabolic stress induced by increasing biomass density of conspecifics, it should scale as

$$a_{ii} = -a_{ii,0} m_i^{-\gamma} \tag{8}$$

where a_{ii} is a normalization constant and γ the scaling exponent (but see DeLong, 2014). Below, I show that if γ ranges from ¼ to ½ (which includes the scaling exponent of mass-specific metabolic rate), empirically tenable scaling between body mass and equilibrium biomass abundance across species is seen in model communities. This is similar to the scaling used in a different set of body size parameterizations of the LV model by

Table 1 Parameters of the Body Size-Based Community Assembly Model and Their Numerical Values

Parameter	Description	Dimensions	Parameter Values
b_i	Mass-specific biomass production rate of the ith basal species	time^{-1}	–
d_i	Mass-specific intrinsic death rate	time^{-1}	–
a_{ij}	Mass-specific search rate of jth consumer for the ith resource	$\text{area} \times \text{time}^{-1}$	–
a_0	Scaling constant for a_{ij}	$\text{area} \times \text{mass}^{0.25} \times \text{time}^{-1}$	10^{-3}–1
b_0	Scaling constant for b_i	$\text{mass}^{0.25} \times \text{time}^{-1}$	10^{-6}–1
d_0	Scaling constant for d_i	$\text{mass}^{0.25} \times \text{time}^{-1}$	10^{-8}–10^{-2}
k	Location parameter for function φ	–	0.001–1000
s	Scale parameter for function φ	–	0.01–0.1
a_{ii}	Mass-specific intraspecific search rate	$\text{area} \times \text{time}^{-1}$	–
γ	Scaling exponent for a_{ii}	–	0–0.25
$a_{ii,0}$	Scaling constant for a_{ii}	$\text{area} \times \text{mass}^{\gamma} \times \text{time}^{-1}$	Depending upon target n at IEE

IEE stands for immigration-extinction equilibrium (see main text). Note that these some of these scaling parameters were also used to calculate the community matrix and stability characteristics of real community food webs (Section 3).

Virgo et al. (2006). This completes specification of the size-based assembly model. Table 1 provides a summary of the parameterizations used for the above scaling relationships.

2.2 Assembly Dynamics

I ignore environmental or demographic stochasticity, and focus on purely interaction-driven stable invasions and species sorting events. Previous studies have theoretically shown how food web structure changes in model communities during assembly though a combination of stable invasions

(establishment of a new immigrant and its trophic links without any extinctions) and species sorting (unstable invasion followed by one or more extinctions) (Bastolla et al., 2005; Fukami, 2004; Pawar, 2009). Specifically, the *i*th immigrant arriving at a community already consisting of m residents will invade and grow in biomass density when rare if the condition

$$\sum_{j\in \mathrm{res}_i} e|a_{ij}|\hat{x}_j > d_i + \sum_{k\in \mathrm{con}_i} |a_{ik}|\hat{x}_k, j, k \in 1, 2, \ldots, m \tag{9}$$

is satisfied (Pawar, 2009; Roughgarden, 1996; Strobeck, 1973). That is, the *i*th immigrant's biomass gain rate through feeding on its set of resources (res_i) must be sufficiently large to offset the loss due to its intrinsic biomass loss rate (d) and consumption exerted upon it by its set of k consumers (con_i), measured when all m resident species are at equilibrium. Note that because the immigrant is rare, intraspecific density dependence a_{ii} (Eq. 8) plays a negligible role in invasion success. This successful invasion will also be a *stable* invasion if subsequently no other species goes extinct, partly determined by the probability of local stability (Pawar, 2009; Tang et al., 2014) of the invaded community. A necessary (but not sufficient) condition for the invasion to be stable is that the new n ($=m+1$) species system is locally asymptotically stable, i.e., the $n \times n$ Jacobian $\boldsymbol{C}$ (the familiar community matrix) with elements,

$$c_{ij} = \left.\frac{\partial(\mathrm{d}x_i/\mathrm{d}t)}{\partial x_j}\right|_{\mathbf{x}=\hat{\mathbf{x}}} = a_{ij}\hat{x}_i, i, j = 1, 2, \ldots, n \tag{10}$$

has all its n eigenvalues $\lambda_i(\boldsymbol{C})$ lying in the negative half of the complex plane, i.e., given that $\lambda_{\max}(\boldsymbol{C}) \equiv \max\{\mathrm{Re}(\lambda_i(\boldsymbol{C}))\}, i = 1, 2, \ldots n$,

$$\lambda_{\max}(\boldsymbol{C}) < 0 \tag{11}$$

must hold (Pawar, 2009; Tang et al., 2014). The element c_{ij} ($i \neq j$) of $\boldsymbol{C}$ represents the population-level effect of a change in the *j*th species' biomass density on the *i*th one, or the dependence of the *i*th species on its own density (if $i = j$), at biomass equilibrium.

Stable invasions (if inequality (9) is satisfied) result in gradual changes in food web structure during assembly, whereas species sorting events (if subsequently, inequality (11) is violated) can cause greater structural upheavals by the extinction of multiple species. Eventually, for a given immigration rate, community assembly reaches quasi-equilibrium where immigrations are approximately balanced by extinctions through failed invasions and species sorting events (immigration-extinction equilibrium, or IEE) (Bastolla et al.,

2005; Fukami, 2004; Pawar, 2009). The condition in Eq. (11) only holds for point equilibria (Allesina and Tang, 2012; May, 1974; Pawar, 2009; Tang et al., 2014). Therefore, I test whether the predictions below (Section 2.3) about effect of size variation on assembly and stability based upon this assumption are more generally valid, using numerical simulations (Section 2.5).

2.2.1 Assembly Without Interactions

To understand the effects of size-mediated interactions on assembly, we can begin by considering the pattern of changes (or lack thereof) in local community body size variation under neutral community assembly—where neither invasion (Eq. 10) nor stability (Eq. 11) matter. This will serve as a null model to test against for the presence of signatures of invasibility and stability constraints during and after assembly.

Assume that the species body mass (size) distribution from which immigrants are drawn can be represented as a probability density function over some body mass range. This function does not merely represent the size distribution of the region to which the community belongs, but is a convolution of the probability density functions of the regional species pool's body size distribution and size-based immigration probability distribution, assuming a relationship between size and dispersal ability (Hein et al., 2012; Jetz et al., 2004). Hence I will refer to this size-distribution as belonging to the 'immigrant pool'. I assume that the probability density function of the sizes in the immigrant pool follows a one-parameter Beta distribution, Beta(1,ω) (Springer, 1979),

$$f_\gamma(\gamma_i) = \omega(1-\gamma_i)^{\omega-1}, \gamma_i \in [0, 1] \tag{12}$$

rescaled to lie between biologically feasible lower and upper log-size limits ($\gamma'_{\min}$ and $\gamma'_{\max}$) of the immigrant pool:

$$\gamma' = \gamma'_{\min} + \left(\gamma'_{\max} - \gamma'_{\min}\right)\gamma \tag{13}$$

Thus, here the random variable $\gamma' = \log(m)$, and the distribution function in Eq. (12) gives the probability of immigration of any species with respect to its log-transformed body size. Note that the logarithm of body mass is being used here purely for convenience. Using the Beta probability, density here has two main advantages. First, it has finite bounds, which allows a precise allocation of minimum and maximum feasible body masses in the model. Second, depending upon the choice of ω, different shapes of size distributions in the immigrant pools (e.g. uniform vs. skewed) can be chosen. The latter factor will be considered in greater detail below.

From the immigrant pool, species are assumed to arrive at the local community at a fixed rate. At each immigration event, the *i*th invader species establishes a trophic link with the *j*th resident species with some probability, which I assume is independent of the body masses of both species because under neutral assembly, the only limitation on species accumulation is immigration rate (ignoring environmental or demographic stochasticity). In this scenario, the log-size distribution of the local community is expected to reflect that of the immigrant pool. I will concentrate on two properties of the local log-size to measure deviations from this null expectation: its mean and kurtosis. The mean of the local community's log-size distribution under neutral assembly would be approximately,

$$\mu_{\text{log-size}} \cong \gamma'_{\min} + \left(\gamma'_{\max} - \gamma'_{\min}\right)\frac{1}{(1+\omega)} \tag{14}$$

(using properties of the Beta(1,γ) distribution). In addition, because log-size distributions tend to be right skewed to different degrees (Allen et al., 2006a), we are interested in skewness of the community's log-size. Again using the properties of the Beta(1, γ) distribution, this is expected to be

$$sk_{\text{log-size}} \cong \frac{2(\omega-1)\sqrt{\omega+2}}{(\omega+3)\sqrt{\omega}} \tag{15}$$

Equations (14) and (15) are only approximations because there is bound to be finite sample error during stochastic immigration from the immigrant pool. The nature of the log-size-ratio distribution under neutral assembly can also be inferred as follows. Assuming that the log-sizes of consumer and resource species follow the same distribution, if trophic links are assumed to be established independent of species body sizes as well as existing links during assembly, the log-size-ratio of each trophic link is the random variable $\gamma'_c - \gamma'_r$ (because $\log(m_c/m_r) = \log(m_c) - \log(m_r)$), with the subscripts 'c' and 'r' denoting consumer and resource species, respectively. We do not need to determine the actual form of this distribution because its mean and kurtosis can be directly calculated. Firstly, because given two independent random variables X and Y, $E(X-Y) = E(X) - E(Y)$,

$$\mu_{\text{log-size-ratio}} \cong 0 \tag{16}$$

Additionally, because the distribution of differences between two independent and identically Beta-distributed random variables is unimodal and symmetric (with upper and lower bounds equal to $\gamma'_{\min} + \gamma'_{\max}$, in our case), again assuming that the size distributions of consumers and resources are

identical, the log-size-ratio distribution must also have approximately zero skewness under neutral assembly, i.e.,

$$sk_{\text{log-size-ratio}} \cong 0 \tag{17}$$

Any deviation from these characteristics of local community log-size and log-size-ratio distributions (Eqs. 14–17) can be attributed to non-random processes during community assembly (which, following random immigration, bias the success of species towards those with particular body sizes). Next, I will show that one such process is non-random species extinctions driven by the stability constraints of multi-species stability.

2.2.2 Assembly with Size-Mediated Interactions

To obtain predictions about non-neutral assembly with size variation, we need to consider the combined constraints of invasibility (Eq. 9) and stability (Eq. 11). First, because both invasibility and stability depend upon resident species' equilibrium biomass abundances ($\hat{x}$'s) we need to consider whether and how equilibrium biomasses themselves depend upon body size in the LV model, as is typically seen in local communities (Cyr et al., 1997a; Leaper et al., 1999). In Appendix A, I show that while deriving this relationship is analytically intractable for arbitrary community size n, it can be found numerically that the above body mass based LV model yields equilibrium biomass densities that scale across species as

$$\hat{x}_i = x_0 m_i^{\nu} \tag{18}$$

where x_0 is the intercept and depending upon the parameters ω and k,

$$\nu = z\gamma - c \tag{19}$$

with z lying between 0.5–0.6 and c between 0.1–015 (see Appendix A). Thus, if γ lies between 0.25 and 0.5, ν lies between 0 and 0.25, which is consistent with data from local communities as well as theory (Cyr et al., 1997a; Leaper et al., 1999; Reuman et al., 2009; Sheldon et al., 1977).

Armed with the scaling of equilibrium abundance, we can now proceed. At the early stages of assembly, because n is small and local stability constraints weak (Pawar, 2009; Tang et al., 2014), the success of each immigrant is dependent mainly on its ability to invade as determined by inequality (9). By substituting Eqs. (4)–(7) and (18) into (9), we get,

$$em_i^{-0.25} \sum_{j \in \text{res}_i} \varphi_{ji} m_j^{\nu} > (d_0/a_0 x_0) m_i^{\beta-1} + \sum_{k \in \text{con}_i} m_k^{-0.25+\nu} \varphi_{ik}, \quad j,k \in 1,2,\ldots,m \tag{20}$$

That is, smaller species are more likely to invade because they tend to have higher mass-specific biomass uptake and production rates (from the negative scaling of these quantities), provided they are able to establish a sufficient number of trophic links with appropriate size-ratios (the function φ) to grow in biomass density when rare. Thereafter, we need to consider how size variation affects local stability during assembly following every successful invasion. For this, I use a previous result for a measure of trophic link strength directly relevant to local stability (Pawar, 2009):

$$\bar{\underline{c}}_{ij} = |a_{ij}| \sqrt{e\hat{x}_i \hat{x}_j} \tag{21}$$

(where i consumes j). Each $\bar{\underline{c}}_{ij}$ is the geometric mean of the pair of coefficients (a_{ij}, a_{ji}) associated with each interspecific interaction, and is proportional to the biomass transfer rate from resource to consumer. Now, substituting Eqs. (5), (6) and (18) into (21), we have the approximate scaling of trophic link strengths:

$$\bar{\underline{c}}_{ij} \cong a_0 m_i^{-0.25} \varphi_{ij} x_0 \sqrt{e m_i^{\nu} m_j^{\nu}} \tag{22}$$

(where j consumes i). However, because local stability is defined relative to the strengths of the diagonal elements of the community matrix (intraspecific density dependences at biomass equilibrium) (see Pawar, 2009; Tang et al., 2014) which also scale with body size (Eq. 8), the scaling of the $\bar{\underline{c}}_{ij}$'s by themselves do not provide sufficient information to understand their effects on community stability. So we need a measure that considers effects of the $\bar{\underline{c}}_{ij}$'s relative to the diagonal elements of $\boldsymbol{C}$. The destabilizing effect of the $\bar{\underline{c}}_{ij}$'s is inversely related to the strengths of the diagonal elements (the c_{ii}'s) of the community matrix $\boldsymbol{C}$, which themselves scale as (combining Eqs. 8, 18 and 19):

$$c_{ii} \cong x_0 a_{ii,0} m_i^{\nu-\gamma}$$

Then, using the result that local stability is inversely related to the quantity $\sum_{i,j=1}^{n} \bar{\underline{c}}_{ij}$ (also see Tang et al., 2014 for an analogous result), the impact of the jth immigrant's successful invasion on stability during assembly can be measured as the ratio of the sum of the strengths of the new trophic link strengths added to the system, over the new diagonal element (intraspecific interference),

$$\frac{\sum_{i\in \mathrm{res}_j}\bar{\zeta}_{ij}}{c_{jj}} \cong \frac{a_0 m_j^{-0.25}\sqrt{e m_j^{\nu}}\sum_{i\in \mathrm{res}_j}\varphi_{ij}\sqrt{m_i^{\nu}}}{a_{jj,0}m_j^{\nu-\gamma}} \tag{23}$$

where res_j is the set of resource species of the new immigrant. Smaller the ratio in Eq. (23), weaker the impact of the new consumer on community stability. The effects of the immigrant's vulnerability (all the new trophic links in which it is the resource) are not included in Eq. (23), because they can be absorbed into the analogous terms of its consumer species. Simplifying Eq. (23) gives,

$$\frac{\sum_{i\in \mathrm{res}_j}\bar{\zeta}_{ij}}{c_{jj}} \cong \frac{a_0\sqrt{e}\sum_{i\in \mathrm{res}_j}\left(\varphi_{ij}m_i^{\nu/2}\right)}{a_{jj,0}m_j^{\frac{\nu}{2}-\gamma+\frac{1}{4}}} \tag{24}$$

Equation (24) indicates that if $\gamma \geq 0.25+\nu/2$, potentially destabilizing effects of the higher mass-specific trophic link strengths associated with smaller species will be counterbalanced by their stronger intraspecific density dependence. Note here that ν itself also increases as a fraction of γ (Eq. 19), and hence it is expected to be >0 for $\gamma \geq 0.25$. If $\gamma = 0.25$, as might be expected from metabolic considerations, the effects of increasing mass-specific biomass acquisition and production rates are canceled out by the biomass loss due to negative intraspecific density dependence. In that case, the denominator of Eq. (24) *increases* with body mass, and larger species tend to be relatively stabilizing. Also, irrespective of its body mass, the stability impact of an immigrant is determined by the terms in the numerator in Eq. (24): the size-ratios (the function φ) associated with its trophic generality (number of res_j's), and provided that $\nu > 0$, the body sizes of these resource species.

Across the range of possible size-ratios over an empirically feasible range of body sizes (see Section 3), Fig. 2 compares the distribution of search rates (a_{ij}'s), trophic link strengths ($\bar{\zeta}_{ij}$'s) and the ratio in Eq. (24) for two different values of γ. Three salient features of the a_{ij}'s are immediately evident from Fig. 2A: (i) they decrease at either extremes of body mass difference, (ii) increase with decrease in body mass of either species (i.e. for a given size-ratio, the peak values—the 'hottest' zones—lie towards the upper left corner of the figure) and (iii) decrease more rapidly at extreme upper values of size-ratios compared to lower extreme values (the hottest zones lie slightly above the size-ratio = 1 line). While (i) is a result of the symmetric unimodality of φ_{ij} (Eq. 7), (ii) and (iii) result from

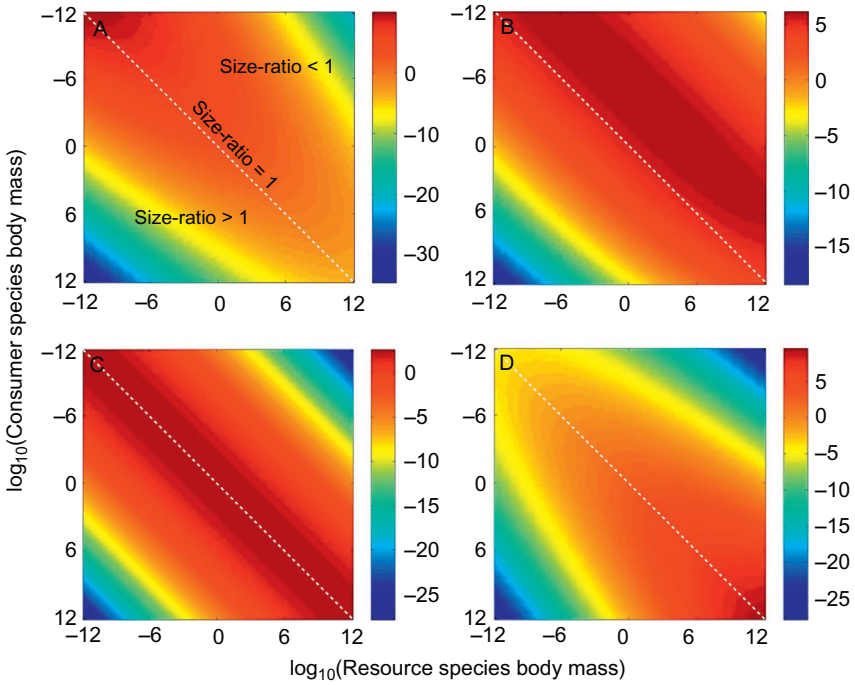

Figure 2 The body size dependence of interspecific trophic interactions across 12 orders of magnitude variation in consumer and resource species' body masses: (A) the variation in search rate (a_{ij}, Eq. 5), (B) trophic link strength ($\bar{\zeta}_{ij}$, Eq. 22, for $\nu = 0.25$), (C) the stability ratio (Eq. 24, for generality = 1), and (D) the same stability ratio for $\nu = 0.25$. Note that $\nu = 0$ and 0.25 correspond approximately to $\gamma = 0.25$ and 0, respectively (Appendix A). All these measures are shown in the log scale to facilitate visual interpretation, and for $k = 1$ and $s = 0.1$. Changing k would change the location of the size-ratio = 1 line, while increasing (decreasing) s would increase (decrease) spread of the measures around k. The values of the allometric scaling constants a_0, and $a_{ii,0}$ are irrelevant here and were arbitrarily set to 1, and e to 0.5.

the scaling of intrinsic biomass production rates (Eqs. 3 and 6), which decrease with size.

These features of mass-specific interaction strengths are consistent with previous such body size-based models (Brose et al., 2006b, 2008; Yodzis and Innes, 1992). Figure 2B shows that if $\nu > 0$ (the case of $\nu = 0.25$ is shown), when the effects of equilibrium biomasses are added to the a_{ij}'s, the resulting trophic link strengths reduce the bias of the interaction strengths towards smaller sized organisms (the hottest zones extend further along the size-ratio = 1 line towards the bottom right corner of the figure), while increasing

the bias towards extreme upper values of size-ratios (the hottest zones lie further above the size-ratio = 1 line). Finally, Fig. 2C and D show that as expected from the body size-scaling composition of the ratio in Eq. (24), for the two extreme values of γ (0.25 and 0.5), the effects of the mass-specific biomass production scaling are either perfectly negated (Fig. 2C), or overwhelmed (Fig. 2D) (because ν increases linearly with γ; Eq. 19). In other words, in the former case (Fig. 2C), the potentially destabilizing effects of smaller body-sized species are negated (the hottest zone becomes a ridge across the entire size-ratio = 1 line), while in the latter (Fig. 2D), larger body-sized species actually become more destabilizing (the hottest zone shifts to the bottom right hand corner along the size-ratio = 1 line). Moreover, the more rapid decline in interaction strengths and trophic link strengths at extreme upper values of size-ratios compared to lower extreme ones is no longer seen—cooler areas are larger below the size-ratio = 1 line in Fig. 2A–B are no longer larger. These analytical insights can now be used to generate predictions of the effect of body size variation on community assembly.

2.3 Predictions for Size-Driven, Interaction-Mediated Assembly

As assembly proceeds, species' generalities tend to increase as more links are established, and therefore the probability of local stability decreases because the numerator in Eq. (24) overwhelms the denominator. Hence, successful invasions are now more often followed by species sorting events, and so while relatively small sized species continue to invade more successfully, the constraints on trophic link strengths have increased. At such a stage, the numerator of Eq. (24) has to be mitigated for the growing number of species to coexist stably. This is possible if, during assembly, irrespective of the size of the consumer, trophic link strength can be weakened by deviation from peak values of the function φ_{ij} (at size-ratio = k) and if $\nu > 0$ (i.e. at least weak increase of equilibrium biomass with body size) by an decrease in the size of the resource species it feeds on (the terms inside the sum of the numerator). These two conditions can simultaneously be satisfied only if the consumer has trophic links with size-ratios >0. Because their higher invasibility will have favored species in the small end of the spectrum of the immigrant pool's body size at the earlier assembly stages, size-ratios will inherently tend to increase because the later immigrants will be on average larger than the residents. Thus two patterns should

emerge during assembly, which as also predicted signatures of size-mediated assembly:

(i) *A negative correlation between a consumer's trophic level and its size-ratios*, and linked to this,

(ii) *A positive correlation between a species' size and its trophic level.*

Predictions **(i)** and **(ii)** can be measured by correlation coefficients (specified below), and will be denoted by $r(TL, \text{size-ratio})$ and $r(TL, \text{size})$, respectively. Note that if community assembly is hierarchical such that later immigrants tend to be consumers rather than resources, occupying higher trophic levels, signatures **(i)** and **(ii)** will be stronger because this will predispose the relatively larger later immigrants towards becoming consumers of resident species. Hence the following interdependency between food web structural signatures of stability constraints are predicted **(i)** $\leftrightarrow$ **(ii)**, i.e., an increase in consumer species' body size and size-ratios with trophic position (measured by $r(TL, \text{size})$ and $r(TL, \text{size-ratio})$, respectively) will be positively correlated (Fig. 5).

I now consider how size and size-ratio distributions change concurrently with predictions **(i)** and **(ii)** above. Firstly, as mentioned above, species with small body sizes are expected to invade with greater success because of their inherently superior rate of mass-specific biomass uptake and production. This is especially true when species richness is low and stability constraints are weak (invasibility constraints dominate community stability constraints). Hence, the local log-size distribution is expected to deviate from the null one in the direction of small body sizes at the early stages of assembly. So $\mu_{\text{log-size}}$ will become increasingly smaller than that expected from neutral assembly (Eq. 14), and skewness of the size distribution $sk_{\text{log-size}}$ higher (more positive, or right-skewed) than that in Eq. 15). At the same time, because trophic link strengths are strongest at size-ratio = 1 (Fig. 2C and D), species will be more successful in invading by feeding on those similar to them in size, and $\mu_{\text{log-size-ratio}}$ and $sk_{\text{log-size-ratio}}$ should initially stay around 0 (the null values, Eqs. 16 and 17). As assembly proceeds, because relatively larger species experience increasingly fare better at invading stably (for reasons explained in prediction **(ii)** above), as the community approaches IEE, $\mu_{\text{log-size}}$ and $sk_{\text{log-size}}$ should decrease at a decreasing rate.

Thus, the invasibility (energetic requirement for initial establishment) of individual species and the stability requirements of

multi-species stable coexistence 'pull' the local size distribution in opposite directions during assembly. Thus, the following two additional predictions can be made about the signatures of dynamically constrained assembly on community size and size-ratio distributions:

(iii) *An asymptotic decrease in* $\mu_{\text{log-size}}$ *and increase in* $sk_{\text{log-size}}$ *during assembly, culminating in smaller and larger values, respectively, of these measures at IEE relative to those of the immigrant pool's size distribution.*

(iv) *An asymptotic increase in* $\mu_{\text{log-size-ratio}}$ *during assembly, culminating in a larger value at IEE relative to that of the immigrant pool's size-ratio distribution.*

It is important to note that as in the case of the assembly signatures **(i)** and **(ii)** above, changes in size-ratios are dependent on assembly sequence or pattern. An increase in $\mu_{\text{log-size-ratio}}$ is possible because the local $\mu_{\text{log-size}}$ progressively decreases relative to that of the immigrant pool; hence if interactions are established more or less randomly with respect to body size, $\mu_{\text{log-size-ratio}}$ is bound to increase (because the species arriving from the immigration pool will be on average larger than those in the local community). Obviously, if later immigrants tend to be consumers with greater probability (occupy higher trophic levels), this effect will be magnified. On the other hand, if assembly is completely non-hierarchical such that each immigrant is equally likely to be a consumer or resource, even if an increase in the $\mu_{\text{log-size-ratio}}$ is favored by stability constraints, it may change little from the null expectation of 0 (Eq. 16) irrespective of the local log-size. Also, although the null expectation for $sk_{\text{log-size-ratio}}$ is 0 (Eq. 17), the current theory cannot predict the direction in which a deviation from it may be expected—this will be investigated numerically below.

2.4 Simulations

I evaluated the above predictions about the emergence of non-random food web structural features (signatures) using numerical simulations of community assembly based on the size-based LV model. For this I used the following three-step community assembly algorithm (Pawar, 2009):

- *Immigration*. Beginning with the establishment at least one basal species, at 1000 time step intervals, a species population was introduced at an extinction-threshold biomass abundance x_e. Each immigrant species was generated by sampling a body size from the Beta(1,ω) distribution introduced in Eq. (12). Inter- and intraspecific interaction parameters were determined by body sizes (Eqs. 3–8).

- *Trophic linking*. Upon colonization, the *j*th immigrant established a trophic link to the *i*th pre-existing one with a connectance probability p_c. For each assembly simulation, conditional upon p_c, a 'vulnerability probability' p_v ranging between 0.5–1 was set: $p_v = 0.5$ meant that the *j*th immigrant was equally likely to be a resource or a consumer of the *i*th resident species (provided it was not basal), while $p_v = 1$ meant that the *j*th immigrant could only be a consumer.
- *Interaction-driven extinction*. After immigration, the augmented system was numerically integrated forward for 1000 time steps, during which most populations either reached a non-zero equilibrium size or went extinct. A species was considered extinct and deleted from the system if its density dropped below x_e, or decreased during this period.

This algorithm was iterated till the system reached IEE. Simulations were performed in Matlab using the Runge–Kutta one-step solver ode45. During each assembly simulation run, changes in key size-related community characteristics ($\mu_{\text{log-size}}$, $\mu_{\text{log-size-ratio}}$, $sk_{\text{log-size}}$, $sk_{\text{log-size-ratio}}$) were measured at 1000-time step intervals (coinciding with the interval for numerical integration). The method used to calculate trophic level is described in Pawar (2009). Simulation parameters were chosen as follows (again, see Pawar, 2009):

- e was fixed at 0.5 for all species, the approximate midpoint of the range reported from empirical data (Brown et al., 2004; Peters, 1986). Values ranging from 0.1 to 1 do not change the simulation results qualitatively.
- p_v was set to 0.9 because this is the midpoint of the range of [0.75–1] that yields communities with structural and dynamical characteristics similar to that of real ones, similar to the niche model (Pawar, 2009). The results do not change qualitatively over the full range of [0.5–1].
- x_e was set to 10^{-20}; the results do not change qualitative for values ranging from 10^{-32} to 10^{-3}.
- The number of basal species was set as a fixed proportion of the total target community size at IEE. All simulation results shown here are for five basal species (~10% of n at IEE, which was 43.1 for $\omega = 1$ and 40.1 for $\omega = 2$; Table 3). The simulation results do not change qualitatively for assembly with fewer or more basal species than this.

In addition, body size-related simulation parameters were chosen as follows (Table 1):

- ω, which determines the shape of the immigrant pool size distribution was varied between 1 (uniform distribution; immigration rate independent of body size) and 2 (power law-like with slope = –2; immigration

probability decreases with body mass). This range of ω was chosen because: (a) empirical data show the distributions of sizes at large spatial scales are right-skewed (Allen et al., 2006a; Clauset and Erwin, 2008), probably partly driven by speciation rate, which appears to follow a negative power law relationship with body size (Dial and Marzluff, 1988; Kozlowski and Gawelczyk, 2002; Marzluff and Dial, 1991), possibly linked to metabolic scaling (Allen and Gillooly, 2006; Allen and Savage, 2007; Allen et al., 2006b) and, (b) dispersal ability should increase with body size (Hein et al., 2012; Peters, 1986). Only considering (a) means that ω should be >1; choosing $\omega = 2$ sets a reasonably high upper limit to this size bias in immigration. Considering (b) means that the effect of (a) may be somewhat negated due to dispersal ability. However, because speciation within the local community also adds to the effective bias towards immigration by smaller species, it is unlikely that (b) can overwhelm the effects of (a). Hence, $\omega = 1$, which yields the uniform distribution expected if the effects of (a) and (b) exactly cancel out, is a reasonable lower limit to the immigration rate bias.

- The log-body mass range $[\gamma'_{\min}, \gamma'_{\max}]$ was chosen to be [–12,12] because this is approximately the range of species' log-body masses observed across empirical communities (Brose et al., 2006a) (also see Fig. 7).
- k was chosen to vary randomly between 10^{-3} and 10^{3} with uniform probability (consumers 1000 times smaller to 1000 times larger than resources), which covers most of the range considered to be 'optimal' (in the sense of viable or evolutionarily stable strategy for the consumer) in previous studies on consumer–resource interactions (Cohen, 2008; Weitz and Levin, 2006), and accommodates potential differences in k across the most common trophic interaction types seen in food webs (i.e. predator–prey, herbivore–plant and parasitoid–host) (Brose et al., 2006a).
- The parameter s was set to 0.1; however, varying it between a wide range (0.05–0.5) does not change the results (simulation results not shown, but see Appendix B).
- The allometric constants b_0 and d_0 were chosen to be 1 and 0.002, respectively, consistent with the observation that baseline birth or production rate is typically two orders of magnitude higher than mortality rate (Brown et al., 2004; Peters, 1986).
- The search rate scaling constant a_0 was varied between 10^{-3} and 1 based upon recent empirical results (Pawar et al., 2012)—the results shown

here are for $a_0 = 1$. Other values in this range do not change the results qualitatively.

- $a_{ii,0}$ was chosen according to the target mean n at IEE; larger values give larger feasible communities (May, 1974; Pawar, 2009; Tang et al., 2014).

2.5 Results

2.5.1 Signatures of Dynamically Constrained Assembly on Size and Size-Ratio Distributions

For both extremes of shapes of the regional log-size distributions ($\omega = 1$ or 2; dashed lines in Fig. 4A and C), Fig. 3A and B shows that as expected, both $\mu_{\text{log-size}}$ and $sk_{\text{log-size}}$ deviate from the null values rapidly, respectively, increasing and decreasing asymptotically, converging on heavily skewed size and symmetric size-ratio distributions (Fig. 4, Table 2). Also, because immigration is strongly dominated by small bodied species for $\omega = 2$, these deviations from the null expectations are proportionally higher. This proportional difference in deviation from the null expectation may be regarded

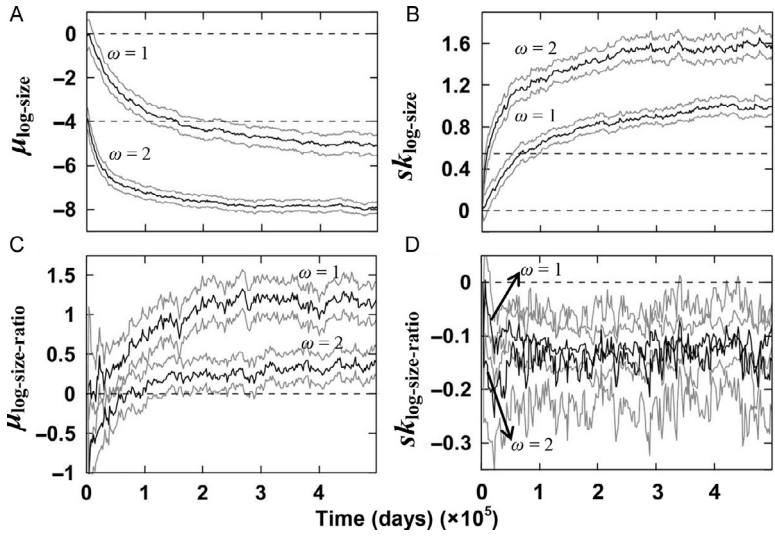

Figure 3 Changes in the log-size and log-size-ratio distributions of model communities during assembly. Mean values with 99% confidence intervals (grey lines) across 150 simulation runs over 400,000 time steps are shown for mean and skewness of the log-size (A and B) and size-ratio distributions (C and D). Each plot compares the trajectories for the two extreme values of ω, with the dashed lines showing the null values of distributional characteristics (Eqs. 14–17). These trends are for the same communities shown in Fig. 4.

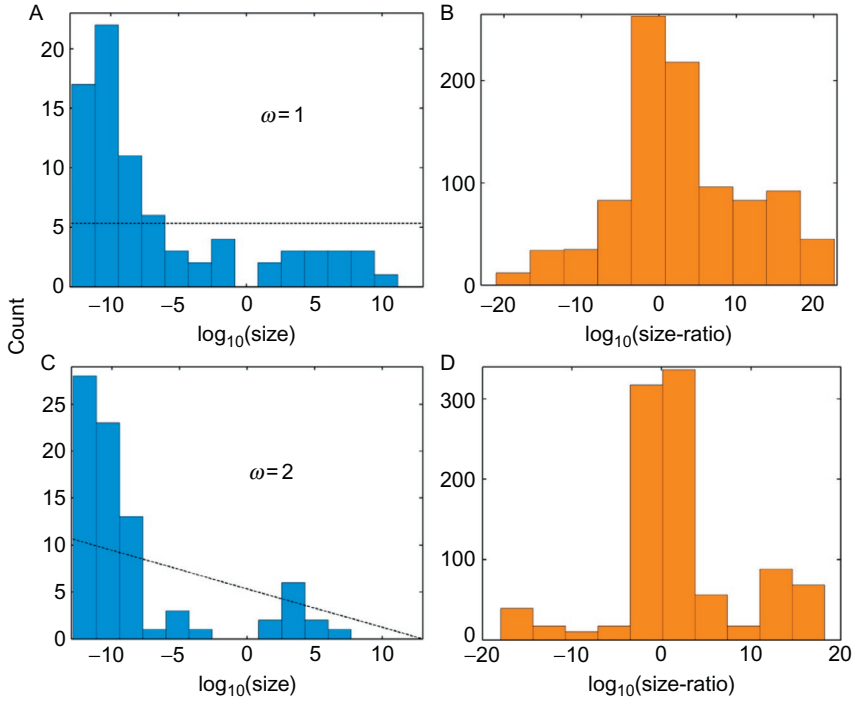

Figure 4 Size distributions (A and C) and the associated size-ratio distributions (B and D) in two different model communities at IEE assembled with $\omega = 1$ (upper panel) and $\omega = 2$ (lower panel). The dashed lines in the size distribution plots show the distribution expected if assembly had been fully neutral (no interactions) and without sampling error.

Table 2 Various Food Web Signatures of Dynamical Constraints on Model Size-Structured Communities at Immigration-Extinction Equilibrium (IEE)

Signatures of Dynamical Constraints	Assembly Type (Distribution of Immigrant Body Sizes)	
	$\omega = 1$ ($n = 43.1 \pm 5.6$)	$\omega = 2$ ($n = 40.1 \pm 5.0$)
$\mu_{\text{log-size}}$	100% (-5.63 ± 1.29)	100% (-7.69 ± 1.11)
$sk_{\text{log-size}}$	100% (1.07 ± 0.36)	100% (1.58 ± 0.47)
$\mu_{\text{log-size-ratio}}$	100% (3.06 ± 1.08)	93.3% (1.56 ± 0.15)
$r(TL, \text{size})$	48% (0.54 ± 0.09)	48% (0.56 ± 0.1)
$r(TL, \text{size-ratio})$	68% (0.31 ± 0.10)	84% (0.31 ± 0.13)

The mean species richness (±SD in parentheses) at IEE for each assembly type is shown in the header row. For each structural feature, the tabulated values give the percentage of 150 model food webs that showed the expected relationship, along with the mean value (±SD) of the measure in parentheses. For size and size-ratio distribution characteristics (rows 1–3), the signature of dynamical constraints was considered significant if a deviation in the expected direction from the null value (Eqs. 14–17) was seen. For measures that are correlation coefficients (rows 4–5) (Spearman's rank correlation), the signature was considered significant if two-tailed $p < 0.01$.

as the 'neutral' component of the log-size distribution. That is, under assembly unconstrained by interactions, the relative difference between the two distributions would be the same, even if their absolute $\mu_{\text{log-size}}$ and $sk_{\text{log-size}}$ values were different from those under dynamically-constrained assembly.

In the case of the log-size-ratio distribution as well, the effects of dynamically constrained assembly were as expected from the above theory—on average, $\mu_{\text{log-size-ratio}}$ increases asymptotically (Fig. 3C). For $\omega = 2$, $\mu_{\text{log-size-ratio}}$ starts off well below the null value (dashed line). This is because invasion success of the first few basal species is independent of their body size as they lack consumers (assuming there is no competition between basal species). However, invasibility of the first consumers feeding on these basal species decreases with body size. For $\omega = 2$, there is already a bias towards migration of small species, and hence $\mu_{\text{log-size-ratio}}$ will tend to <0 (consumer smaller than resource) initially. Even after the early stages of assembly, however, $\mu_{\text{log-size-ratio}}$ values for $\omega = 2$ remain below those seen for $\omega = 1$, which, as in the case of the size distribution, indicates that sufficiently strong immigration bias can counteract dynamical constraints on assembly. In the case of $sk_{\text{log-size-ratio}}$ on the other hand, both ω values result in a similarly weak negative deviation from the null value of 0 (note that this null value will be the same irrespective of ω), indicating that skewness of the log-size-ratio distribution may not carry a strong signature of dynamically constrained assembly. Also, the increase in $\mu_{\text{log-size-ratio}}$ during assembly indicates an overall shift of size-ratios away from the hottest zones lying along the size-ratio = 1 line towards the cooler zones (weaker interactions) below the line in Fig. 2C.

Table 2 shows that in all predicted signatures (Section 2.3, Fig. 6) of dynamically constrained assembly, a high incidence (high percentage values) of the expected signatures is seen irrespective of ω. Moreover, even in the case where the incidences were low, trends in the opposite direction were not seen. For example, in the case of increase in body size with trophic level $r(TL, \text{size})$, although only 48% of the communities show the expected relationship, none of the remaining ones showed a significant relationship in the opposite direction (decrease in body mass with trophic level). Finally, Fig. 5 shows that the interdependencies between the two signatures are as predicted in Section 2.3. Changes in other, non-body size-related food web structural features were similar to those seen during assembly based on the LV model (see Pawar, 2009), and are not shown here.

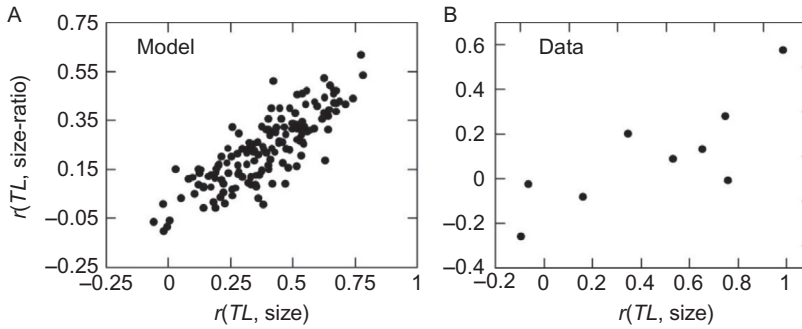

Figure 5 The interdependence between two trait-based food web structural signatures of constrained assembly across (A) 150 model communities at immigration-extinction equilibrium (IEE) and (B) the nine real communities. The relationships are strong and highly significant (A: $p < 0.0001$, $R^2 = 0.68$; B: $p < 0.02$, $R^2 = 0.63$). The model results are for communities assembled at $\omega = 1$. The strengths of these signatures across model communities are summarized in Table 2 and for real communities in Table 6.

3. DATA

I analyzed nine relatively high quality datasets using data-selection criteria that ensured only those communities which have a relatively well-resolved tropic interaction structure were chosen (see Pawar, 2009 for details). In particular, these criteria eliminated community datasets that had been subjected to substantial *a priori* taxonomic aggregation. I did not aggregate taxa into 'trophospecies', wherein taxa with highly similar or identical sets of consumer and resource species are treated as the same functional unit (i.e. two or more network nodes are collapsed into one). Apart from the fact that developing objective criteria for trophospecies is a difficult task (Yodzis, 1988), the use of this approach in the current study is undesirable for two reasons. First, the trophospecies approach has been used mainly in 'static' structural studies of food webs wherein only the presence-absence of trophic links are studied, and not the associated interaction strengths (see Allesina et al., 2008 and references therein). In contrast, this study is focused on effects of invasibility and dynamical stability during food web assembly—hence, even if two species have identical consumers and resources, they are unlikely to have identical strengths of interactions across the links, and hence are not dynamically equivalent. Second, the complete structure of the quantified food web is necessary for analyzing the stability of the community, and collapsing nodes into trophospecies can give a distorted view of the

community's dynamical characteristics. Nine food webs were selected (Table 3). In the GC community, only one of the six subcommunities (Clmown1) was chosen because they all had similar food web structural properties (connectance, average trophic degree and food chain length were more similar between these communities than between them and others).

Whenever only data on a species' linear dimension was available, it was converted using allometric relationships of the form: mass $= a$ (length)^b. The parameters a and b were varied according to broad taxonomic groups (typically at the level of class and order) (Enquist and Niklas, 2001; Peters, 1986) (Table 4). In the case of certain groups such as worms and coelenterates, no meta-analyses were available. In these cases, the parameters of groups with similar body form and mass density were used (for example legless herpetofauna for worms). Of the community datasets that had body mass (instead of length) data to begin with, most consisted of at least a few species whose mass information was derived by the original authors using such length-to-mass conversions. The EW community consists of 391 taxa including a number of animal groups for whom length-mass scaling information are unavailable, and whose body forms preclude the use of scaling parameters of other groups (e.g. coelenterates and anthozoans) (Brose et al., 2005). Hence length, instead of mass data, was used for this community.

Clearly, taxonomic class- or order-wide use of the same length-mass scaling parameter is bound to increase the inherent noise in such data; this is exacerbated by the substitution of parameters for groups without information. However, as will be discussed further below, across local communities, $>$20 orders of magnitude interspecific body mass variation is seen, with each local community having been sampled for at least six orders of magnitude variation (Fig. 7). I expect these errors to be mitigated by this wide size variation.

3.1 Data Analyses

3.1.1 Signatures of Dynamically Constrained Assembly

Four size-related properties of real communities that I was able to compare with the predicted signatures of dynamically constrained assembly (Section 2.3) are illustrated in Fig. 6. Given that data on the regional species pool for each of these communities is unavailable, it was not possible to test for significant different of $\mu_{\text{log-size}}$ or $sk_{\text{log-size}}$ from null expectations. Therefore, I only tested whether $\mu_{\text{sk-size}}$ was positively skewed as predicted by the theory (part of prediction **(iii)**, Section 2.3). A test of significant skewness

Table 3 The Empirical Community Datasets Used to Test Theoretical Predictions About Signatures of Dynamical Constraints on Food Web Structural Characteristics

Community Name	General Habitat	Description	Trophic Link Method[a]	Body Mass Method[b]	Data Sources	Food Web Characteristics				
						n	C_T	$\bar{G}$	$\bar{T}_c$	O_{deg}
Broadstone stream (BS)	Aquatic (stream)	Spring-fed acidic headwater stream, Sussex, UK	1, 2	2	Brose et al. (2005) and Woodward et al. (2005)	28	0.37	15.3	4.6	0.81
Caribbean sea (CS)	Aquatic (marine)	Benthic and pelagic communities from surface to 100 m depth	3	2, 3	Bascompte and Melian (2005)	248	0.11	13.5	4.6	0.45
Eastern Weddell Sea (EW)	Aquatic (marine)	Antarctic shelf	1, 2	2, 3	Brose et al. (2005)	391	0.02	9.5	2.9	0.21
Grand Cariçaie marsh (GC)	Terrestrial	Marsh dominated by *Cladietum marisci*, Lake Neuchâtel, Switzerland	1, 3, 4	1, 2, 3	Brose et al. (2005) and Cattin et al. (2004)	163	0.16	24.0	4.8	1.05
Mill Stream (MS)	Aquatic (freshwater)	Lowland chalk stream, Dorset, UK	2	2	Brose et al. (2005)	74	0.14	8.2	1.2	0.03
Scotch Broom (SB)	Terrestrial	Community on *Cytisis scoparius*, Berkshire, UK	1, 2	1, 2, 3	Brose et al. (2005), Cohen et al. (2005) and Memmott et al. (2000)	153	0.03	10.2	3.2	0.14
Skipwith pond (SP)	Aquatic (freshwater)	Large acidic pond, North Yorkshire, UK	1, 2, 3	1, 2	Brose et al. (2005) and Warren (1989)	33	0.61	17.8	4.1	0.58

Continued

Table 3 The Empirical Community Datasets Used to Test Theoretical Predictions About Signatures of Dynamical Constraints on Food Web Structural Characteristics—cont'd

Community Name	General Habitat	Description	Trophic Link Method	Body Mass Method	Data Sources	Food Web Characteristics				
						n	C_T	$\bar{G}$	$\bar{T}_c$	O_{deg}
Tuesday lake (TL)	Aquatic (freshwater)	Small, mildly acidic lake, Michigan, USA	1, 2	1, 2	Brose et al. (2005), Cohen et al. (2003) and Jonsson et al. (2005)	72	0.15	12.3	3.8	0.18
Ythan estuary (YE)	Estuarine	Ythan river mouth, Scotland	1, 3, 4	1, 2, 3	Hall and Raffaelli (1991) and Leaper and Huxham (2002)	79	0.09	5.7	3.2	0.56

The abbreviation of each community's name used in subsequent tables and figures are shown in parentheses. The last four columns show some key food web structural characteristics (Pawar, 2009): species number (n), undirected connectance (C_T), average generality of consumers ($\bar{G}$), average trophic chain length ($\bar{T}_c$), and omnivory degree (O_{deg}). Body mass is expressed in grams throughout this study.

[a]1: Direct observations (lab or field), 2: Gut/stomach content analysis (typically, predators), feeding trials (typically, predators) or rearing (typically, parasitoids), 3: Published account, 4: Unpublished sources (including dissertation theses and Internet sites).

[b]1: Direct measurement, 2: Length-mass regression (see Table 4), 3: Published account, 4: Unpublished sources (including dissertation theses and Internet sites).

Table 4 Parameter Values Used for Converting Length (m) to Wet Mass (g) Using Scaling Models of Species in Different Taxonomic Groups Across Communities Using the Relationship Mass $= a$ Length^b

General Taxonomic Category	a	b	References
Plants	27	3.79	Niklas and Enquist (2001)
Fish	10600	2.57	Peters (1986)
Worms*	720	3.02	Peters (1986)
Mammals	14000	3.23	Peters (1986)
Birds	7390	2.74	Peters (1986)
Legless herpetofauna	720	3.02	Peters (1986)
Legged lizards	28000	2.98	Peters (1986)
Frogs	181000	3.24	Peters (1986)
Arachnids*	8800	2.62	Peters (1986)
Crustaceans*	8800	2.62	Peters (1986)
Insects (terrestrial and aquatic)	8800	2.62	Peters (1986)
Planktonic crustaceans	80	2.1	Peters (1986)
Algae	5.8	1.9	Peters (1986)
Other planktonic invertebrates*	80	2.1	Peters (1986)

For animals, the scaling for snout-vent length was used. Parameters for arachnids, crustaceans and some planktonic vertebrates were substituted from those of other groups with similar body form and density (marked with an asterisk).

without knowledge of what the null expectation should (the real value taken by ω in Eq. (15) be would be pointless in this scenario. Also note that $sk_{\text{log-size-ratio}}$ is not expected to show a strong signature of dynamically constrained (text following prediction **(iv)**, Section 2.3). For all other signatures, i.e., a positive $\mu_{\text{log-size-ratio}}$, $r(TL, \text{size})$ and $r(TL, \text{size-ratio})$, I tested for significance of the measure by calculating the approximate one-tailed p-value as the proportion of 2000 size-randomized communities that had a value of the measure greater than that of the observed, original community. The bivariate relationships $r(TL, \text{size})$ and $r(TL, \text{size-ratio})$ were calculated using the Spearman rank correlation coefficient.

Size randomizations were performed in two ways: full and partial. Under full randomization, species' body masses were randomly permuted while keeping the food web structure intact. This is easily done by permuting body

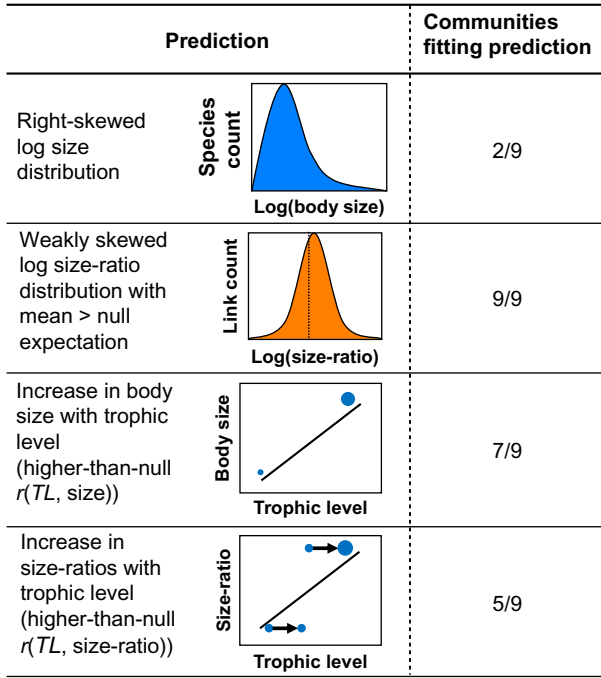

Figure 6 A graphical overview of the predicted signatures of dynamically constrained assembly on community size structure and observed fits of data to them. The term 'null expectation' refers to the values of characteristics expected under purely neutral trophic linking and assembly. Each filled circle in a figure indicates a single consumer species' node in the food web, with arrows indicating their trophic links with its resources. The size of a circle and the thickness of an arrow represent, respectively, species body mass and interspecific interaction strength. Also see Table 5.

masses across species. Under partial randomization, body masses were randomly permuted only within basal and non-basal species (i.e. trophic level 1 vs. all others). This additional, conservative method of randomization was used because it maintains the body mass ranges of basal and non-basal species, which have been found to show consistent patterns within habitat types, and may be driven by historical, biogeographical and environmental factors rather than the trophic dynamics of the system (Brown and Gillooly, 2003; Hildrew et al., 2007).

3.1.2 Community Stability Properties

I also tested whether the observed communities had indeed self-organized during assembly in a manner that enhanced their stability, by examining whether the observed system was more likely to be locally (Hurwitz) stable

(Eq. 11) than an ensemble of randomized counterparts. For this, I calculated the community matrix $\boldsymbol{C}$ with elements $c_{ij} = a_{ij}\hat{x}_i$ using species' body mass information by substituting interspecific and intraspecific interaction rates calculated according to Eqs. (5)–(8) with parameter values from the ranges shown in Table 1. As in the simulation results, the following empirical results do not change qualitatively over these parameter ranges. I chose to fix the parameter k at 1 (maximum consumption intensity when consumers and resources are equal in size) for simplicity—Appendix B shows that the results are robust to a wide range of variation in this parameter. The value of s was chosen as follows. The function φ_{ij} (Eq. (7)) approaches zero more and more rapidly as s increases. As $s \to 0.1$, consumption rate falls to zero within the range of the size-ratios observed across the nine real communities Fig. 7, hence values larger than this are unfeasible because if a size-ratio is observed, no matter how extreme, it must be associated with some level of consumption. On the other hand, the consumption rate function becomes flat as $s \to 0$, and the effects of size-ratios on trophic link strengths are eliminated. Hence, s was set at 0.05, the midpoint of these two extreme values of s. Appendix B shows that the results are remarkably robust to variation in both k and s.

The additional parameter needed to calculate a c_{ij}—equilibrium biomass density—was calculated according to the scaling Eq. (18). For this, the scaling exponent ν was chosen to range between 0 and 0.25, which is consistent with data from local communities (Cyr et al., 1997a,b; Leaper et al., 1999; Tang et al., 2014), as well as the range of exponents predicted by current theories that combine size-metabolic scaling with trophic interactions (Loeuille and Loreau, 2006; Marquet et al., 1995; Rossberg et al., 2008; Woodward et al., 2005). The normalization constant x_0 rescales all the elements of $\boldsymbol{C}$ and was arbitrarily chosen to be 1—a wide range of values, between 0.001 and 100, do not change the results qualitatively.

The exponent γ, which determines the scaling of mass-specific biomass loss rate due to intraspecific interactions, was also chosen to lie between 0 and 0.25, which accommodates density dependence ranging from being independent of species body masses ($\gamma = 0$), to that expected from the scaling of mass-specific metabolic rate ($\gamma = 0.25$) (see Section 2). Finally, for each combination of values of ν and γ, the value of the scaling constant a_{ii} was chosen to be the minimum value across species that would guarantee that the system was locally stable—any nontrivial community matrix can be rendered stable by increasing the magnitudes of the negative diagonal elements (Allesina and Tang, 2012; May, 1974; Pawar, 2009; Tang et al., 2014).

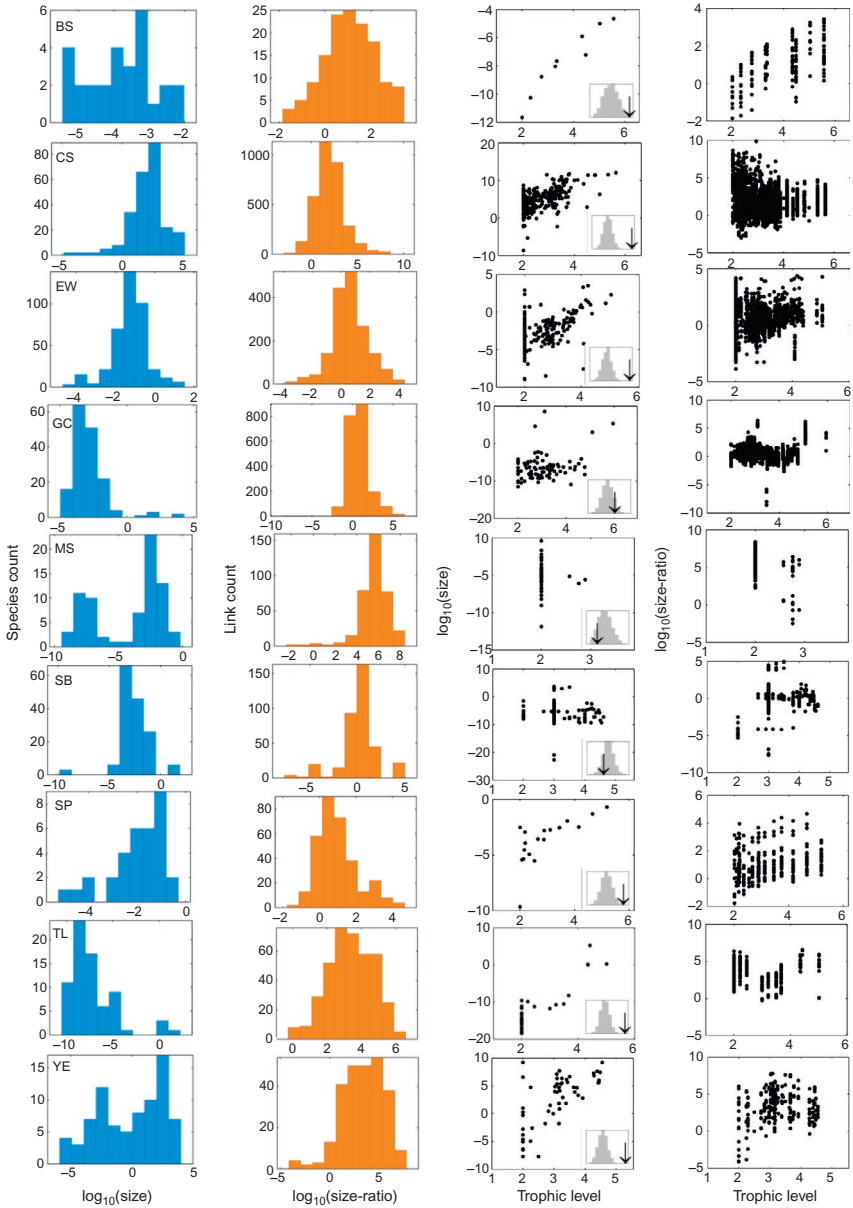

Figure 7 Food web characteristics across nine empirical communities that are expected to show signatures of size-constrained community assembly. Each row of figures represents the four features that should show signatures of size-driven assembly constraints for a particular community (Fig. 6). The histograms embedded in the third column of figures show the location of the correlation coefficient $r(TL, \text{size})$ with respect to the distribution of the coefficients from 2000 size-randomizations of the community. Fits of all these different features to theoretical predictions are summarized in Fig. 6. For the EW community, body size measure is length, not mass.

This was done by first calculating $\boldsymbol{C}$ and assigning a value of c_{ii} that was arbitrarily large (such that the system was locally stable). The value of c_{ii} was then gradually decreased until $\lambda_{\max}(\boldsymbol{C})$ became positive, thus giving the minimal value needed to make the system Hurwitz stable. This minimal value of c_{ii} was then used across the community matrices of the randomized counterparts of the community.

3.2 Results

3.2.1 Signatures of Dynamically Constrained Assembly

Figure 7 shows the four key community food web characteristics across the nine communities, and Table 5 summarizes the incidence and significance of structural signatures expected from dynamically constrained assembly. Only the results for the more conservative partial randomizations are shown. Full randomizations yielded consistently lower p-values, as expected.

Table 5 shows that the majority of communities indeed show the two signatures that underlie the distributions of size and size-ratios—consistently positive and significant $r(TL, \text{size})$ and $r(TL, \text{size-ratio})$. Only in Mill Stream and Scotch Broom are the opposite trends seen. This is not surprising because as shown in Section 2.3, these features are strongly dependent on hierarchical assembly, wherein later species are more likely to be consumers

Table 5 Signatures of Size-Mediated Dynamical Constraints in Real Communities

	Signatures of Size-Based Dynamical Constraints			
Community	$sk_{\text{log-size}}$	$\mu_{\text{log-size-ratio}}$	$r(TL, \text{size})$	$r(TL, \text{size-ratio})$
BS	−0.07	1.07*	0.98*	0.58*
CS	−1.17	2.02*	0.53*	0.09*
EW	−0.1	1.61*	0.34*	0.20*
GC	2.32*	0.74*	0.16*	−0.08
MS	−0.49	5.53*	−0.10	−0.26*
SB	−1.03	0.09	−0.07	−0.03
SP	−1.19	0.99*	0.75*	0.28*
TL	1.69*	3.38*	0.76*	−0.01
YE	−0.38	3.36*	0.65*	0.13*

Significant measures are flagged (*). For $sk_{\text{log-size}}$, a positive value of the skew was deemed significant, while for the other three measures, one-tailed significance is at $p < 0.05$, based upon a randomization test (see main text for more details). Note that MS shows a significant correlation in the opposite direction.

than resources. In the case of the MS community, trophic link sampling appears to be poor, with only the average trophic level value being only 1.2 (Table 3). I consider the effects of sampling inadequacy on the results in Appendix C. In the case of the SB community, on the other hand, the observed reversal of the expected pattern suggests a fundamentally different body size organization, as expected for a terrestrial community based on a single primary producer species, and with the largest proportion of parasitoid–host links among the nine communities. The predicted correlation between $r(TL, \text{size})$ and $r(TL, \text{size-ratio})$ (Section 2.3) seen in model communities is also seen in the empirical ones (Fig. 5).

The expected right skew of log-size distributions is seen in only two communities (Table 5). Indeed, Fig. 7 shows that the nine communities have a variety of log-size distributions, including two that are clearly bimodal (YE and MS). Consistent with theoretical predictions (Section 2.3) the mean of the log-size-ratio distributions tends to be >0 (biased towards size-ratios >1) (Table 5, Fig. 7). Moreover, the communities show a $\mu_{\text{log-size-ratio}}$ that is higher than that expected by (partially) random trophic linking given the observed size distribution (neutral assembly). Interestingly, the mean $\mu_{\text{log-size-ratio}}$ values of most of the communities lie within or close to the range seen for the model communities assembled using the LV model (i.e. 3.06 ($\pm$1.08 SD) and 1.56 ($\pm$0.15 SD), depending upon the parameter ω; Table 2). Also, all the observed log-size-ratio distributions show at most weak left skewness (see Fig. 7), with skewness values ranging from -1.9 (MS community) to 0.81 (SP community). This is consistent with the theoretical prediction (Section 2.3) that skewness of the log-size-ratio distribution is expected to show a weak signature of stability constraints. In Appendix C, I show that sampling in adequacy partly explains why size and size-ratio distributions show weaker agreement with the predictions than $r(TL, \text{size})$ and $r(TL, \text{size-ratio})$.

3.2.2 Stability of Observed versus Size-Randomized Communities

Table 6 summarizes the local stability properties of the nine communities (proportion of 2000 size-randomized food webs that had $\lambda_{\max}(\boldsymbol{C})$ smaller than that of the observed one). As might be expected, the $\lambda_{\max}(\boldsymbol{C})$ of the observed communities deviates more strongly from those of fully randomized webs compared to the partially randomized ones. Overall, irrespective the scaling of equilibrium biomasses (parameter ν) or the intraspecific density dependence (γ), the observed size and size-ratio structure of the empirical food webs clearly tend to endow some level of stability. Moreover, most

Table 6 The Proportion of 2000 Randomized Community Food Webs that Were More Stable Than the Empirically Observed One (Had Smaller $\lambda_{max}(\boldsymbol{C})$), Given Various Values of the Scaling Exponents ν (Mass-Biomass Scaling) and γ (Scaling of Mass-Specific Intraspecific Density-Dependent Biomass Loss)

			Community								
Randomization	γ	ν	**BS**	**CS**	**EW**	**GC**	**MS**	**SB**	**SP**	**TL**	**YE**
Part	0	0	0	0.04	0.01	0	0	0.38	0	0	0.05
		0.25	0	0.64	0.13	0	0.008	0.47	0	0	0.67
	0.25	0	0.20	0.001	0.36	0.40	0.20	0.25	0.12	0.32	0.51
		0.25	0.58	0.13	0	0.49	0.53	0	0.15	0.02	0.93
Full	0	0	0	0.03	0.004	0	0	0.29	0	0	0.001
		0.25	0	0.55	0.08	0	0.005	0.37	0	0	0.19
	0.25	0	0.06	0	0.39	0.35	0.03	0.08	0.06	0.33	0.14
		0.25	0.35	0.19	0	0.48	0.60	0	0.10	0.002	0.86

Note that in most cases, $\lambda_{max}(\boldsymbol{C})$ values are $\ll 1$, that is, the observed webs, with their non-random size structure, are more stable.

of the cases where the stability of observed webs is no better or worse than random (values ≥ 0.5), appear when equilibrium biomasses are assumed to scale strongly with body mass ($\nu = 0.25$). This value of ν is expected under the energetic equivalence rule, but is rarely observed in real communities (Cyr et al., 1997a; Leaper et al., 1999; Marquet et al., 1995; Reuman et al., 2009; Sheldon et al., 1977).

Thus overall, these results provide strong evidence that the observed local food webs show signatures of dynamically constrained assembly in their body size structure.

4. DISCUSSION

In summary, I find that species' body sizes and consumer–resource size-ratios are likely to change systematically with assembly, which, depending upon the pattern or sequence of assembly, may be reflected in **(i)** increase in body size with trophic level, **(ii)** increase in consumer–resource size-ratio with trophic level, and eventually at extinction immigration equilibrium, **(iii)** a strongly right-skewed distribution of body sizes and (iv) a symmetric distribution of size-ratios with mean >1 (or >0 in log space). Most importantly, all these signatures of dynamically constrained assembly are likely to emerge irrespective of the distribution of body sizes (trait values) in the immigration pool because invasibility and stability constraints exert a strong filter on interaction strengths and thus body sizes and size-ratios. Because species' body sizes are relatively easy to measure in the field, the quantification of these signatures offers a simple method to gauge the importance of non-neutral processes underlying the assembly and persistence of real communities.

The predicted increase in sizes with trophic level due to stability constraints is a pattern that is commonly observed in natural communities, especially aquatic ones (Hildrew et al., 2007; Riede et al., 2011). This study appears to be the first to show that assembly dynamics can contribute to this aspect of community food web structure. Previous models have mainly invoked species' metabolic constraints and principles of biomass transfer across trophic levels, without the explicit consideration of interaction driven community assembly dynamics (Brown and Gillooly, 2003; Brown et al., 2004; Cohen, 2008).

The distribution of size-ratios along trophic levels is another signature of dynamically constrained assembly, and can explain why the traditional Eltonian paradigm (Elton, 1927) of invariance of size-ratios with trophic

level does not always, or even typically, hold (Brose, 2010; Cohen and Fenchel, 1994; Riede et al., 2011). My results also differ from that of Jonsson and Ebenman (1998), who concluded that size-ratio ratios should decrease with trophic level due to stability constraints. Our results differ for two reasons. First, Jonsson and Ebenman only studied predator prey interactions with size-ratios >1. Second, they did not consider the context of community assembly and the tradeoff between invasibility and stability. All these factors act together to result in a gradual increase in size-ratios during assembly, culminating in a positive correlation between tropic level and size-ratio, as predicted (Section 2.3), demonstrated numerically (Section 2.5) and supported empirically (Section 3.2).

From the perspective of trait variation, I have shown that irrespective of the distribution of immigration probability with respect to body size, a right-skewed unimodal log-size distribution emerges through species invasion and extinction dynamics driven by interspecific trophic interactions. The skewness and unimodality of this distribution is a result of the tradeoff between the higher invasibility of smaller body-sized consumer species at early stages of assembly due to their higher mass-specific metabolic rate, and the stabilizing effects (in terms of local stability of the community) of invasion by larger sized species during later stages. That such a unimodal, right-skewed log-size distribution, which is often reported in the empirical literature (Jonsson et al., 2005; Leaper et al., 2001; Siemann et al., 1999; Stead et al., 2005), emerges due to stability constraints is an intriguing result. The origin of the local community's size distribution is an enduring problem in biology, and a variety of explanatory hypotheses have been proposed in the past. Only a small subset of these include interspecific interactions (Allen et al., 2006a). The theory developed in this paper combines the features of three classes of previous size distribution models that exclusively consider, (a) metabolic restrictions of resource use by species' individuals (e.g. Brown et al., 1993), (b) size-based constraints on speciation and dispersal (e.g. Etienne and Olff, 2004) and (c) interspecific interactions (e.g. Hutchinson, 1959).

However, I found little support for a predominance of right-skewness in empirical log-size distributions, which should be the result of the same processes that drive the emergence of the weighted generality-based food web structural signatures. I argue that this lack of right-skewness can be partly attributed to inadequate taxonomic sampling—there is strong evidence that size distributions become more right skewed as the inherent taxonomic bias towards larger organisms is mitigated (Blackburn and Gaston, 1994). Indeed,

studies on local communities that have high taxonomic resolution typically find a right-skewed log-size distribution (Allen et al., 2006a) (these could not be included in this study due to lack of trophic interaction data). Also, as shown in Section 2, the local size distribution is dependent upon the size distribution of the immigration pool, and other factors such as the size dependence of speciation and immigration rate. It is currently difficult to determine whether these differ across the different communities studied here. But then why do taxonomic sampling biases also not render $r(TL, \text{size})$ and $r(TL, \text{size-ratio})$ undetectable? This is not surprising because taxonomic sampling *per se* does not affect detection of food web structure as much (Goldwasser and Roughgarden, 1997; Martinez et al., 1999).

The size-ratio distribution emerges concurrently with that of the size distribution. The interest in the effect of stability constraints on the distribution of size-ratios in local communities as a whole appears to have arisen relatively recently (Brose et al., 2006b; Emmerson and Raffaelli, 2004; Jonsson and Ebenman, 1998; Otto et al., 2007), perhaps partly due to increasing availability of food web datasets with body size information (Barnes et al., 2008; Brose et al., 2005). These studies have mainly focused on size-ratios that maximize the fitness or persistence of consumer–resource species pairs (Vasseur and McCann, 2005; Weitz and Levin, 2006; Yodzis and Innes, 1992) without considering assembly dynamics or multi-species coexistence stability. My results support previous conclusions that the size-ratio distribution is constrained by community stability constraints (Brose et al., 2006b; Emmerson and Raffaelli, 2004; Jonsson and Ebenman, 1998). However, it differs from these studies in that it includes a larger spectrum of size-ratios <1, such as those between parasitoids or parasites and their hosts (but see Otto et al., 2007). The fundamental mechanism that interlinks size-ratios to community dynamics identified by those studies and this one are the same (the stabilizing effect of the relatively weaker mass-specific interaction strengths associated with larger size-ratios). However, this study shows that because the size-ratio distribution is tightly linked to that of the community's sizes, it is difficult to separate the feedback between size-ratios *per se* and community stability. For example, assuming that trophic linking probability (p_c) is independent of body sizes, changes in the size-ratio distribution will partly reflect the realized trophic linking due to differences in the sizes of the immigrant pool and the local community.

While I did find support for the effect of stability constraints on the size-ratio distribution, I also found evidence that these apparent fits to the theoretical predictions were *overestimated* by trophic link sampling biases against

size-ratios ≤ 1 (Appendix C). Such a bias is understandable because of the practical difficulties associated with detecting interactions wherein consumers are much smaller than their resources (such as parasites and parasitoids). Nevertheless, biases in current food web datasets may seriously hinder our understanding of community stability dynamics because a spectrum of potentially important trophic interactions (mainly with size-ratios <1) remains undersampled.

In general, while the incidences of different signatures (in terms of the percentage of communities showing the expected patterns in each feature) were consistent with those seen in model communities (cf. Table 2), their strengths (e.g. values of the correlation coefficients) lay at or beyond the lower ends of those of model communities. This is not surprising, given the multiple sources of noise inherent in community datasets, combined with the fact that the model communities were assembled without spatial or temporal environmental variation, both of which are expected to have strong effects on real communities. It is also possible that there is a greater influence of biogeographically neutral processes such as immigration and stochastic extinction (which would weaken signatures of interaction driven stability constraints on food web structural features) than what was simulated. I also tested for the possibility that some or all of the observed signatures were artefacts of trophic link sampling bias (Appendix C). I found that this was not the case; in fact, there was some evidence that the strengths and incidences of the observed signatures may actually be underestimated due to sampling bias.

5. CONCLUSIONS

In this paper, I have studied the effect of species' average adult body size, a trait that constrains the magnitudes of mass-specific trophic interactions, on local community assembly. The results show that under biologically feasible assumptions about allometric constraints and community assembly patterns (or assembly sequences), certain body size and consumer–resource size-ratio distributions are likely to emerge due to a combination of which trait values facilitate invasion, and which allow multi-species stable coexistence. I also find strong empirical support for the theoretical results. Body size allows individual level properties to be mapped on to population interactions in assembly dynamics, providing fresh insights into the dynamical organization of natural communities and ecosystems. This is particularly important because the use of species body size data

provides a valuable tool to decipher the rather daunting complexity of dynamically assembling natural communities.

ACKNOWLEDGEMENTS

I would like to thank Catalina Estrada, Matthew Leibold, Daniel Bolnick, Lauren Myers, Timothy Keitt, Evan Economo, Richard Law, Sahotra Sarkar and Van Savage for comments, and suggestions that improved this work immensely. I would also like to thank Jennifer Dunne for providing the community food web data.

APPENDIX A. THE SIZE SCALING OF SPECIES' EQUILIBRIUM ABUNDANCES

The vector of equilibrium biomass densities $\hat{x}$ can be found by solving the system

$$-\boldsymbol{A}\boldsymbol{x}=\boldsymbol{b}-\boldsymbol{d} \tag{A1}$$

where x is the vector of biomasses (x_i), b of the biomass production rates, d of the density-independent biomass loss rates, and A the $n \times n$ matrix of interaction coefficients. Using Cramer's rule to solve equation, the equilibrium density of the ith species' population can be expressed as a ratio of determinants,

$$\hat{x_i} = -\frac{\det(\boldsymbol{A_i})}{\det(\boldsymbol{A})} \tag{A2}$$

where A_i is the is the matrix formed by replacing the ith column of A with the vector b–d. Now, Leibniz's formula states that for any $n \times n$ matrix $\boldsymbol{Z}$, $\det(\boldsymbol{Z}) = \sum_{\sigma \in \mathrm{P_n}} \mathrm{sgn}(\sigma) \prod_{i=1}^{n} z_{i\sigma(i)}$, where P_n is the set of all possible permutations of the integers 1 to n, and $\mathrm{sgn}(\sigma)$ denotes the signature of the permutation product σ. Thus, while the solution to Eq. (A1) is analytically tractable, deciphering the body size scaling of $\hat{x}$ for an arbitrary community size (n) is not, because both the numerator as well as denominator of Eq. (A2) consist of sums and differences of the $n!$ different permutations of elements (taken n at a time) of the matrices $\boldsymbol{A_i}$ and $\boldsymbol{A}$, respectively. Hence instead, I determine the relationship numerically by examining the biomass abundances of species in model communities at IEE. The results are shown in Fig. A1. In general, there is a tight linear relationship between ν and γ of the form $\nu = z\gamma + c$ with z lying between 0.5–0.6 and c between 0.1–015, depending upon the choice of the parameter k (log-size-ratio at which consumption intensity peaks). There appears to be no strong dependence of the scaling between ν and γ on ω (distribution of body sizes in the immigrant

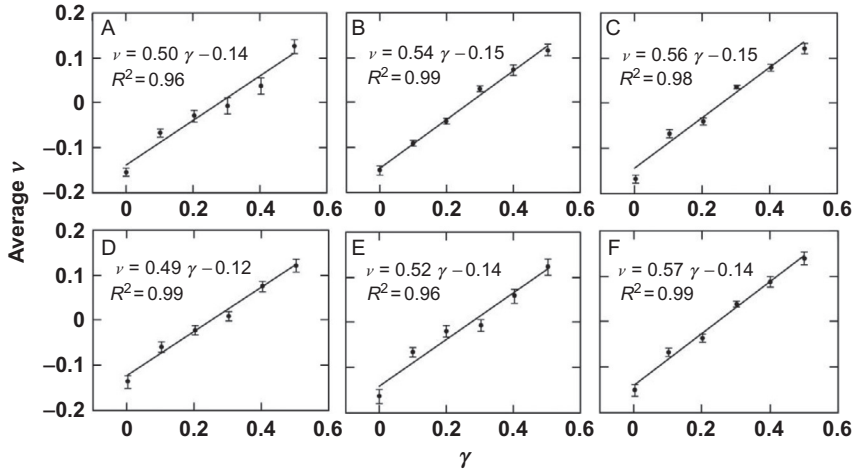

Figure A1 The body size dependence of species' equilibrium biomass abundances ($\hat{x}$'s) in model communities. Each plot shows changes in average ν with increasing values of γ. Each value of average ν (±99% confidence intervals) for a given γ was calculated from 100 replicated communities at IEE. The least-squares regression line and the associated equation are shown for each plot. All the regressions are highly significant ($p < 0.0001$). Plots (A–C) are for $\omega = 1$ but with orders of magnitude increase in k (10^{-3}, 1 and 10^{3}, respectively, i.e., size-ratios for peak consumption intensity ranging from 0.001 to 1000), and (D–F) for $\omega = 2$ and the same range of k. Assembly simulation methodology is described in the main text.

pool). Variation in other non-allometric assembly model parameters (see main text) does not change the linearity of this scaling or the range of z and c (results not shown).

APPENDIX B. PARAMETER SENSITIVITY

B.1 Metabolic Scaling Parameters

The fact that I have used a metabolic scaling exponent of ¾ throughout this study might suggest that this scaling exponent relationship is truly universal. Deviations from this exponent can be found within many taxonomic groups (DeLong et al., 2010; Glazier, 2005; Peters, 1986). However, this relationship does hold well across taxonomic groups spanning large orders of magnitude variation in body sizes, which is typically how local communities are composed. Accordingly, the analysis above also encompasses >20 orders of magnitude variation in body size. I have also not included body temperature dependence into the allometry of metabolism for parameterizing the LV model (Dell et al., 2011, 2014; Gillooly et al., 2001; Pawar et al., 2015). This

can be justified to some extent because the vast majority of species in local communities belong to the same metabolic category (ectotherms), so temperature change would similarly change inter- and intraspecific interaction rates across species, leaving the qualitative results unchanged (assuming all species had identical sensitivity to temperature change). Nevertheless, because temperature-dependence can differ significantly between interacting species (Dell et al., 2014), a more realistic body size-based network assembly model should include temperature dependence to account for climatic variation across space, or the effects of climate change.

Another potential problem is the assumption that species' intraspecific density dependence scales with mass according to Eq. (8). I am unaware of any empirical data on the actual scaling of intraspecific density dependence with body mass. The values ¼–½ for γ were chosen because they yield empirically feasible values for the scaling exponent of equilibrium biomasses (Appendix A). Hence, until relevant empirical data become available, the model developed in this study should be viewed for what it is: a possible set of mechanisms for the emergence of biomass scaling in local communities. Note also that as long as equilibrium biomasses in local communities scale with ν between 0 and 0.25, and empirical data strongly support this (Brown and Gillooly, 2003; Leaper et al., 1999), the results of this study remain qualitatively unchanged.

B.2 Scaling of Search Rates

Because variation in encounter rates can effectively change the location of the peak (k) of the consumption intensity function φ_{ij} (Eq. 7), here I examine sensitivity of the results to variation in its two parameters (k and s). In the main text, I explained the reasons for fixing k (the size-ratio at which consumption rate peaks) and s (the speed with which consumption rate declines away from k) at 1 and 0.05, respectively, instead of varying them according to the type of trophic interaction, habitat or the types of organisms involved. To examine the sensitivity of the observed signatures of stability constraints on food web structure to variation in these parameters, here I examine the key signature of dynamically constrained assembly in empirical/communities, $r(TL, \text{size})$ as follows. Using the methods described in the main text, I recalculated $r(TL, \text{size})$ for each of 100 logarithmically spaced values for k between 10^{-3} and 10^{3} (consumer 1000 times smaller to 1000 times larger than resource) and 100 linearly placed values for s between 0.01 and 0.1. This range for k covers most of the size-ratios considered to be 'optimal'

(in the sense of viable or evolutionarily stable strategies for consumers) in previous studies on body size-based consumer–resource interactions (Cohen, 2008; Weitz and Levin, 2006), and accommodates potential differences in k across the most common trophic interaction types seen in food webs (i.e. predator–prey, herbivore–plant and parasitoid–host) (Brose et al., 2006a). The upper range for s (0.1) was chosen because as $s \to 0.1$, consumption intensity falls to zero within the range of the size-ratios observed across the nine real communities (Fig. 7). Hence, values larger than this are unfeasible because if a size-ratio is observed, no matter how extreme, it *must* be associated with some level of biomass acquisition by the consumer. The lower limit of s (0.01) was chosen as some value arbitrarily higher than 0 because φ_{ij} becomes flat as $s \to 0$ and the effects of size-ratios on trophic link strengths are eliminated (Fig. 2). The simulations results are also similarly robust to considerable variation in k and s (Table 1).

Figure B1 shows the resulting variation in the strength of $r(TL, \text{size})$. Clearly, this signature and the others correlated with it (Figs. 5 and 6) are robust to changes in k, with the correlation coefficient remaining similar across its entire range, as long as $s < 0.05$ or so. As $s \to 0.1$ however, the signatures either become stronger or weaker, depending upon the community and the value of k. This is the effect of elimination of the trophic links associated with extreme size-ratios (because φ_{ij} becomes zero), which strongly biases the interaction data towards trophic links with size-ratios close to k. However, in none of the cases are sign of the relationship reversed, and the value of the correlation coefficient remains within a narrow range across the entire parameter space. Also, the SB community shows a different pattern from the others; whereas the detectability of the correlation signatures becomes weaker as k decreases all the others, it in fact peaks at $k = 10^{-3}$ in the SB community. This is because SB is the only community with a significant number of host-parasitoid interactions. Thus, changing k according to the interaction type makes the signatures of constrained assembly more detectable—k should in fact be $\ll 0$ in host–parasitoid interactions. Similarly, k is typically ≥ 0 in predator–prey interactions, which dominate all communities other than SB, thus explaining why strengths of the signatures increase towards $k = 10^3$ in them. Thus overall, the strengths of the observed signatures, and the main conclusions of this study would be much stronger if trophic link-specific values for k were used. Another community that stands out is EW, where the strengths of both signatures peak at $k = 1$ ($\log_{10}(k) = 0$ in the figures); this is it is the community with the most balanced size-ratio distribution (in terms of the representation of size-ratios <1; Fig. 7).

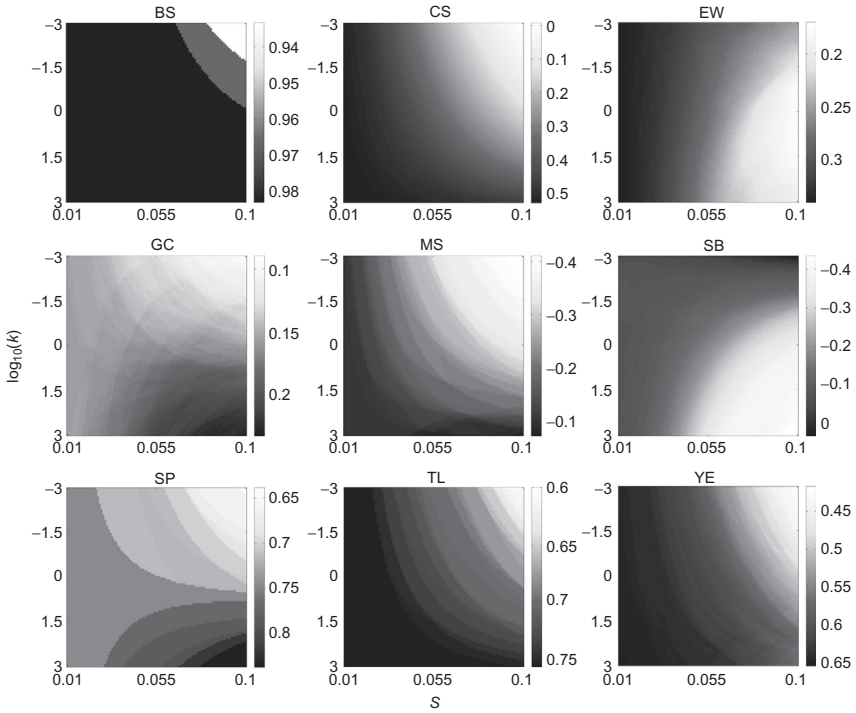

Figure B1 The effect of variation in the parameters *k* and *s* on the predicted measure *r*(*TL*, size), a key food web structural signature of dynamically constrained assembly, across nine real communities.

APPENDIX C. DO SAMPLING BIASES AFFECT THE EMPIRICAL RESULTS?

Here, I consider to what extent the above empirical results are affected by sampling inadequacies. This is important because collecting trophic interaction data are an extremely difficult and time labor-intensive task, and at best it is possible to quantify only a subset of the interaction network of any local community (Berlow et al., 2004; Goldwasser and Roughgarden, 1997; Martinez et al., 1999). Errors in community food web datasets arise from two main sources: lack of taxonomic sampling and lack of adequate trophic link sampling. As discussed above, the former probably affects the observed shapes of size distribution and size-ratio distributions, and potentially, food web structural features as well. However, quantifying this source of error is beyond the scope of this study because it would require sampling

effort and species accumulation data from each of the local communities. Quantifying sampling inadequacies in trophic link data is a somewhat more tractable proposition, especially because given a sample of species from a local community, the potential distribution of trophic links can be estimated. Furthermore, certain biases in trophic link data are well documented. For example, numerous studies have shown that most food web datasets have an underrepresentation of parasite–host interactions, as well as all trophic interactions where both consumers and resources are small in size (Hechinger et al., 2011; Kuris et al., 2008; Lafferty et al., 2008; Leaper and Huxham, 2002; Memmott et al., 2000; Thompson et al., 2005). Hence here, I consider the effect of trophic link sampling bias on this paper's results.

A number of food web structural features are known to be especially sensitive to inadequate sampling of interactions (Goldwasser and Roughgarden, 1997; Martinez et al., 1999). To obtain a measure of sampling inadequacy across communities, I selected a suite of food web structural characteristics were found to be sensitive to sampling effort by Goldwasser and Roughgarden (Goldwasser and Roughgarden, 1997). These features are connectance (C_T), average generality of consumers ($\bar{G}$), average trophic chain length ($\bar{T}_c$) and omnivory degree (O_{deg}). O_{deg} is the mean of the standard deviations of each consumer species' trophic height (standard deviation of the lengths of all the paths to the species from its basal species; Goldwasser and Roughgarden, 1997; Martinez et al., 1999). Other features such as the number and maximum of trophic chain lengths are also sampling sensitive, but are directly related to one or more of these selected measures, and were not included. Nevertheless, the selected features are still (albeit indirectly) interdependent (for example O_{deg} will typically increase with $\bar{T}_c$); hence, I used a Principal Component Analysis (PCA) to combine them into a single pseudo-variable that can be used as an index of sampling sensitivity. The correlation of strengths of the ostensible signatures of stability constraints across communities with this index would then provide insights into the effects of sampling error. If the signatures become stronger with increasing values of the index, it would suggest that the above results would have been stronger with better sampling. On the other hand, if the signatures become weaker, it would suggest the above results are an artefact of sampling bias.

Data normality is a central assumption of PCA; because the distributions of these food web structural features across communities were somewhat skewed, the data were square-root transformed, which resulted in approximately normal distributions of all four variables (determined using the Lilliefors test). The PCA did indeed result in a single significant component

accounting for 86% of variance (with loadings in the following order: $\bar{T}_c > O_{deg} > C_T > \bar{G}$). The scores of this first component were thereafter used as an index of trophic link sampling inadequacy, with which the correlation of observed strengths of the key signature of dynamically constrained assembly $r(TL, \text{size})$ (Section 2.3; $r(TL, \text{size-ratio})$ is correlated with this, see Fig. 5) across communities was calculated using the spearman rank coefficient. The correlation was weakly positive ($R^2 = 0.14$), but insignificant ($p = 0.16$). At the very least, this indicates that the above results are not an artefact of sampling bias.

I also examined the correlation of $\mu_{\text{log-size-ratio}}$ with trophic link sampling inadequacy. Stability constraints are expected to increase the community's $\mu_{\text{log-size-ratio}}$ (Section 2.3), which should therefore be positively correlated with link sampling inadequacy index if sampling bias decreases the observed strength of this signature. However, this correlation was found to be weakly negative ($R^2 = 0.34$) but insignificant ($p = 0.21$). Nevertheless, this suggests that unlike the food web structural signatures, the observed fit of the $\mu_{\text{log-size-ratio}}$ to theoretical predictions may in fact be affected by sampling bias. In other words, while the observed $\mu_{\text{log-size-ratios}}$ are qualitatively consistent with theoretical predictions, their actual values may be overestimated because of an underrepresentation of links with size-ratios <1 (typically observed in the form of parasite–host, parasitoid–host or herbivore–plant interactions). This conclusion is further supported by the fact that that the skewness of the log-size-ratio distribution is also positively and significantly correlated ($R^2 = 0.67$, $p = 0.009$) with the link sampling inadequacy index. Because a higher positive skewness means an inordinately high concentration of values at the right half of the distribution (where size-ratios >1) this indicates that the sampling bias may in fact be against size-ratios ≤ 1, as has been suggested in recent studies highlighting the lack of data on host–parasite links. This is also supported by the fact that an overwhelming majority ($\sim$90%) of links across the nine communities were of predator–prey interactions, which typically have size-ratios >1.

REFERENCES

Aljetlawi, A.A., Sparrevik, E., Leonardsson, K., 2004. Prey-predator size-dependent functional response: derivation and rescaling to the real world. J. Anim. Ecol. 73, 239–252.

Allen, A.P., Gillooly, J.F., 2006. Assessing latitudinal gradients in speciation rates and biodiversity at the global scale. Ecol. Lett. 9, 947–954.

Allen, A.P., Savage, V.M., 2007. Setting the absolute tempo of biodiversity dynamics. Ecol. Lett. 10, 637–646.

Allen, C.R., Garmestani, A.S., Havlicek, T.D., Marquet, P.A., Peterson, G.D., Restrepo, C., Stow, C.A., Weeks, B.E., 2006a. Patterns in body mass distributions: sifting among alternative hypotheses. Ecol. Lett. 9, 630–643.
Allen, A.P., Gillooly, J.F., Savage, V.M., Brown, J.H., 2006b. Kinetic effects of temperature on rates of genetic divergence and speciation. Proc. Natl. Acad. Sci. U.S.A. 103, 9130–9135.
Allesina, S., Tang, S., 2012. Stability criteria for complex ecosystems. Nature 483, 205–208.
Allesina, S., Alonso, D., Pascual, M., 2008. A general model for food web structure. Science 3, 658–661.
Barnes, C., et al., 2008. Predator and body sizes in marine food webs. Ecology 89, 881.
Bascompte, J., Melian, C.J., 2005. Simple trophic modules for complex food webs. Ecology 86, 2868–2873.
Bascompte, J., Stouffer, D.B., 2009. The assembly and disassembly of ecological networks. Philos. Trans. R. Soc. Lond. B Biol. Sci. 364, 1781–1787.
Bastolla, U., Lassig, M., Manrubia, S.C., Valleriani, A., 2005. Biodiversity in model ecosystems, II: species assembly and food web structure. J. Theor. Biol. 235, 531–539.
Berlow, E.L., et al., 2004. Interaction strengths in food webs: issues and opportunities. J. Anim. Ecol. 73, 585–598.
Blackburn, T.M., Gaston, K.J., 1994. Animal body-size distributions change as more species are described. Proc. Biol. Sci. 257, 293–297.
Brose, U., 2010. Body-mass constraints on foraging behaviour determine population and food-web dynamics. Funct. Ecol. 24, 28–34.
Brose, U., et al., 2005. Body sizes of consumers and their resources. Ecology 86, 2545.
Brose, U., et al., 2006a. Consumer-resource body-size relationships in natural food webs. Ecology 87, 2411–2417.
Brose, U., Williams, R.J., Martinez, N.D., 2006b. Allometric scaling enhances stability in complex food webs. Ecol. Lett. 9, 1228–1236.
Brose, U., Ehnes, R.B., Rall, B.C., Vucic-Pestic, O., Berlow, E.L., Scheu, S., 2008. Foraging theory predicts predator-prey energy fluxes. J. Anim. Ecol. 77, 1072–1078.
Brown, J.H., Gillooly, J.F., 2003. Ecological food webs: high-quality data facilitate theoretical unification. Proc. Natl. Acad. Sci. U.S.A. 100, 1467–1468.
Brown, J.H., Marquet, P.A., Taper, M.L., 1993. Evolution of body-size: consequences of an energetic definition of fitness. Am. Nat. 142, 573–584.
Brown, J.H., Gillooly, J.F., Allen, A.P., Savage, V.M., West, G.B., 2004. Toward a metabolic theory of ecology. Ecology 85, 1771–1789.
Cattin, M.F.M., Bersier, L.F., Banasek-Richter, C., Baltensperger, R., Gabriel, J.P., Banas, C., 2004. Phylogenetic constraints and adaptation explain food-web structure. Nature 427, 835–839.
Clauset, A., Erwin, D.H., 2008. The evolution and distribution of species body size. Science 321, 399–401.
Cohen, J.E., 2008. Body sizes in food chains of animal predators and parasites. In: Hildrew, A.G., Raffaelli, D.G., Edmonds-Brown, R. (Eds.), Body Size: The Structure and Function of Aquatic Ecosystems. Cambridge University Press, Cambridge, UK, pp. 306–325.
Cohen, J.E., Fenchel, T., 1994. Marine and continental food webs: three paradoxes? Proc. R. Soc. B Biol. Sci. 343, 57–69.
Cohen, J.E., Jonsson, T., Carpenter, S.R., 2003. Ecological community description using the food web, species abundance, and body size. Proc. Natl. Acad. Sci. U.S.A. 100, 1781–1786.
Cohen, J.E., Jonsson, T., Müller, C.B., Godfray, H.C.J., Savage, V.M., Muller, C.B., 2005. Body sizes of hosts and parasitoids in individual feeding relationships. Proc. Natl. Acad. Sci. U.S.A. 102, 684–689.

Cyr, H., Downing, J., Peters, R., 1997a. Density-body size relationships in local aquatic communities. Oikos 79, 333–346.
Cyr, H., Peters, R.R.H., Downing, J.J.A., 1997b. Population density and community size structure: comparison of aquatic and terrestrial systems. Oikos 80, 139–149.
Dell, A.I., Pawar, S., Savage, V.M., 2011. Systematic variation in the temperature dependence of physiological and ecological traits. Proc. Natl. Acad. Sci. U.S.A. 108, 10591–10596.
Dell, A.I., Pawar, S., Savage, V.M., 2014. Temperature dependence of trophic interactions are driven by asymmetry of species responses and foraging strategy. J. Anim. Ecol. 83, 70–84.
DeLong, J., 2014. The body-size dependence of mutual interference. Biol. Lett. 10.
DeLong, J.P., Okie, J.G., Moses, M.E., Sibly, R.M., Brown, J.H., 2010. Shifts in metabolic scaling, production, and efficiency across major evolutionary transitions of life. Proc. Natl. Acad. Sci. U.S.A. 107, 12941–12945.
Dial, K.P., Marzluff, J.M., 1988. Are the smallest organisms the most diverse? Ecology 69, 1620–1624.
Economo, E.P., Kerkhoff, A.J., Enquist, B.J., 2005. Allometric growth, life-history invariants and population energetics. Ecol. Lett. 8, 353–360.
Elton, C.S., 1927. Animal Ecology. Macmillan, New York.
Emmerson, M.C., Raffaelli, D., 2004. Predator-prey body size, interaction strength and the stability of a real food web. J. Anim. Ecol. 73, 399–409.
Enquist, B.J., Niklas, K.J., 2001. Invariant scaling relations across tree-dominated communities. Nature 410, 655–660.
Etienne, R.S., Olff, H., 2004. How dispersal limitation shapes species-body size distributions in local communities. Am. Nat. 163, 69–83.
Fahimipour, A.K., Hein, A.M., 2014. The dynamics of assembling food webs. Ecol. Lett. 17, 606–613.
Fukami, T., 2004. Community assembly along a species pool gradient: implications for multiple-scale patterns of species diversity. Popul. Ecol. 46, 137–147.
Giacomini, H.C., Shuter, B.J., de Kerckhove, D.T., Abrams, P.A., 2013. Does consumption rate scale superlinearly? Nature 493, E1–E2.
Gillooly, J.F., Brown, J.H., West, G.B., Savage, V.M., Charnov, E.L., 2001. Effects of size and temperature on metabolic rate. Science 293, 2248–2251.
Glazier, D.S., 2005. Beyond the "3/4-power law": variation in the intra- and interspecific scaling of metabolic rate in animals. Biol. Rev. Camb. Philos. Soc. 80, 611–662.
Goldwasser, L., Roughgarden, J., 1997. Sampling effects and the estimation of food-web properties. Ecology 78, 41.
Hall, S.J.J., Raffaelli, D., 1991. Food-web patterns: lessons from a species-rich web. J. Anim. Ecol. 60, 823–842.
Hechinger, R.F., Lafferty, K.D., Dobson, A.P., Brown, J.H., Kuris, A.M., 2011. A common scaling rule for abundance, energetics, and production of parasitic and free-living species. Science 333, 445–448.
Hein, A.M., Hou, C., Gillooly, J.F., 2012. Energetic and biomechanical constraints on animal migration distance. Ecol. Lett. 15, 104–110.
Hildrew, A.G., Raffaelli, D.G., Edmonds-Brown, R., 2007. Body Size: The Structure and Function of Aquatic Ecosystems. Cambridge University Press, Cambridge, New York.
Hutchinson, G.E., 1959. Homage to Santa Rosalia or why are there so many kinds of animals? Am. Nat. XCIII 145–159.
Jetz, W., Carbone, C., Fulford, J., Brown, J.H., 2004. The scaling of animal space use. Science 306, 266–268.
Jonsson, T., Ebenman, B., 1998. Effects of predator-prey body size ratios on the stability of food chains. J. Theor. Biol. 193, 407–417.

Jonsson, T., Cohen, J., Carpenter, S., 2005. Food webs, body size, and species abundance in ecological community description. Adv. Ecol. Res. 36.
Kleiber, M., 1961. The Fire of Life: An Introduction to Animal Energetics. Wiley, New York.
Kozlowski, J., Gawelczyk, A.T., 2002. Why are species' body size distributions usually skewed to the right? Funct. Ecol. 16, 419–432.
Kuris, A.M., et al., 2008. Ecosystem energetic implications of parasite and free-living biomass in three estuaries. Nature 454, 515–518.
Lafferty, K.D., et al., 2008. Parasites in food webs: the ultimate missing links. Ecol. Lett. 11, 533–546.
Leaper, R., Huxham, M., 2002. Size constraints in a real food web: predator, parasite and prey body-size relationships. Oikos 99, 443–456.
Leaper, R., Raffaelli, D., Letters, E., 1999. Defining the abundance body-size constraint space: data from a real food web. Ecol. Lett. 2, 191–199.
Leaper, R., Raffaelli, D., Emes, C., Manly, B., 2001. Constraints on body-size distributions: an experimental test of the habitat architecture hypothesis. J. Anim. Ecol. 70, 248–259.
Loeuille, N., Loreau, M., 2006. Evolution of body size in food webs: does the energetic equivalence rule hold? Ecol. Lett. 9, 171–178.
Marquet, P.A., Navarrete, S.A.S., Castilla, J.J.C., 1995. Body size, population density, and the energetic equivalence rule. J. Anim. Ecol. 64, 325–332.
Martinez, N.D., Hawkins, B.A., Dawah, H.A., Feifarek, B.P., 1999. Effects of sampling effort on characterization of food-web structure. Ecology 80, 1044–1055.
Marzluff, J.M., Dial, K.P., 1991. Life-history correlates of taxonomic diversity. Ecology 72, 428–439.
May, R.M., 1974. Stability and Complexity in Model Ecosystems. Princeton University Press, Princeton, NJ.
May, R.M., 2009. Food-web assembly and collapse: mathematical models and implications for conservation. Philos. Trans. R. Soc. Lond. B Biol. Sci. 364, 1643–1646.
McCoy, M.W., Gillooly, J.F., 2008. Predicting natural mortality rates of plants and animals. Ecol. Lett. 11, 710–716.
Memmott, J., Martinez, N.D., Cohen, J.E., 2000. Predators, parasitoids and pathogens: species richness, trophic generality and body sizes in a natural food web. J. Anim. Ecol. 69, 1–15.
Niklas, K.J., Enquist, B.J., 2001. Invariant scaling relationships for interspecific plant biomass production rates and body size. Proc. Natl. Acad. Sci. U.S.A. 98, 2922–2927.
O'Dwyer, J.P., Lake, J.K., Ostling, A., Savage, V.M., Green, J.L., 2009. An integrative framework for stochastic, size-structured community assembly. Proc. Natl. Acad. Sci. U.S.A. 106, 6170–6175.
Otto, S.B., Rall, B.C., Brose, U., 2007. Allometric degree distributions facilitate food-web stability. Nature 450, 1226–1229.
Pawar, S., 2009. Community assembly, stability and signatures of dynamical constraints on food web structure. J. Theor. Biol. 259, 601–612.
Pawar, S., Dell, A.I., Savage, V.M., 2012. Dimensionality of consumer search space drives trophic interaction strengths. Nature 486, 485–489.
Pawar, S., Dell, A.I., Savage, V.M., 2013. Pawar et al. reply. Nature 493, E2–E3.
Pawar, S., Dell, A.I., Savage, V.M., 2015. From metabolic constraints on individuals to the eco-evolutionary dynamics of ecosystems. In: Belgrano, A., Woodward, G., Jacob, U. (Eds.), Aquatic Functional Biodiversity: An Eco-Evolutionary Approach. Elsevier, Amseterdam, in press.
Persson, L., Leonardsson, K., de Roos, A.M., Gyllenberg, M., Christensen, B., 1998. Ontogenetic scaling of foraging rates and the dynamics of a size-structured consumer-resource model. Theor. Popul. Biol. 54, 270–293.

Peters, R., 1986. The Ecological Implications of Body Size. Cambridge University Press, Cambridge.
Post, W.M., Pimm, S.L., 1983. Community assembly and food web stability. Math. Biosci. 64, 169–182.
Raffel, T.R., Martin, L.B., Rohr, J.R., 2008. Parasites as predators: unifying natural enemy ecology. Trends Ecol. Evol. 23, 610–618.
Reuman, D.C., et al., 2009. Allometry of body size and abundance in 166 food webs. Adv. Ecol. Res. 41, 1–44.
Riede, J.O., Brose, U., Ebenman, B., Jacob, U., Thompson, R., Townsend, C.R., Jonsson, T., 2011. Stepping in Elton's footprints: a general scaling model for body masses and trophic levels across ecosystems. Ecol. Lett. 14, 169–178.
Rossberg, A.G., Ishii, R., Amemiya, T., Itoh, K., 2008. The top-down mechanism for body-mass-abundance scaling. Ecology 89, 567–580.
Roughgarden, J., 1996. Theory of Population Genetics and Evolutionary Ecology: An Introduction. Prentice Hall, Upper Saddle River, NJ.
Savage, V.M., Gilloly, J.F., Brown, J.H., Charnov, E.L., Gillooly, J.F., West, G.B., 2004. Effects of body size and temperature on population growth. Am. Nat. 163, 429–441.
Schmidt-Nielsen, K., 1984. Scaling, Why is Animal Size so Important? Cambridge University Press, Cambridge; New York.
Sheldon, R.W., Sutcliffe, W.H., Paranjape, M.A., 1977. Structure of pelagic food chain and relationship between plankton and fish production. J. Fish. Res. Board Can. 34, 2344–2353.
Siemann, E., Tilman, D., Haarstad, J., 1999. Abundance, diversity and body size: patterns from a grassland arthropod community. J. Anim. Ecol. 68, 824–835.
Springer, M.D., 1979. The Algebra of Random Variables. Wiley, New York.
Stead, T.K., Schmid-Araya, J.M., Schmid, P.E., Hildrew, A.G., 2005. The distribution of body size in a stream community: one system, many patterns. J. Anim. Ecol. 74, 475–487.
Strobeck, C., 1973. N species competition. Ecology 54, 650–654.
Tang, S., Pawar, S., Allesina, S., 2014. Correlation between interaction strengths drives stability in large ecological networks. Ecol. Lett. 17, 1094–1100.
Thompson, R.M., Mouritsen, K.N., Poulin, R., 2005. Importance of parasites and their life cycle characteristics in determining the structure of a large marine food web. J. Anim. Ecol. 74, 77–85.
Vasseur, D.A., McCann, K.S., 2005. A mechanistic approach for modeling temperature-dependent consumer-resource dynamics. Am. Nat. 166, 184–198.
Virgo, N., Law, R., Emmerson, M., 2006. Sequentially assembled food webs and extremum principles in ecosystem ecology. J. Anim. Ecol. 75, 377–386.
Vucic-Pestic, O., Rall, B.C., Kalinkat, G., Brose, U., 2010. Allometric functional response model: body masses constrain interaction strengths. J. Anim. Ecol. 79, 249–256.
Warren, P.H., 1989. Spatial and temporal variation in the structure of a freshwater food web. Oikos 55, 299–311.
Weitz, J.S., Levin, S.A., 2006. Size and scaling of predator-prey dynamics. Ecol. Lett. 9, 548–557.
Woodward, G., Speirs, D.C., Hildrew, A.G., 2005. Quantification and resolution of a complex, size-structured food web. Adv. Ecol. Res. 36, 85–135.
Yodzis, P., 1988. The indeterminacy of ecological interactions as perceived through perturbation experiments. Ecology 69, 508–515.
Yodzis, P., Innes, S., 1992. Body size and consumer-resource dynamics. Am. Nat. 139, 1151–1175.